Bar-mode instability of a rapidly spinning black hole in higher dimensions: Numerical simulation in general relativity

Masaru Shibata and Hirotaka Yoshino

Yukawa Institute for Theoretical Physics, Kyoto University, Kyoto, 606-8502, Japan
and Department of Physics, University of Alberta, Edmonton, Alberta, Canada T6G 2G7

(Received 3 February 2010; published 18 May 2010)

Numerical-relativity simulation is performed for rapidly spinning black holes (BHs) in a higher-dimensional spacetime of special symmetries for the dimensionality $6 \leq d \leq 8$. We find that higher-dimensional BHs, spinning rapidly enough, are dynamically unstable against nonaxisymmetric bar-mode deformation and spontaneously emit gravitational waves, irrespective of d as in the case $d = 5$ [M. Shibata and H. Yoshino, Phys. Rev. D **81**, 021501(R) (2010).]. The critical values of a nondimensional spin parameter for the onset of the instability are $q := a/\mu^{1/(d-3)} \approx 0.74$ for $d = 6$, ≈ 0.73 for $d = 7$, and ≈ 0.77 for $d = 8$ where μ and a are mass and spin parameters. Black holes with a spin smaller than these critical values ($q_{\rm crit}$) appear to be dynamically stable for any perturbation. Long-term simulations for the unstable BHs are also performed for $d = 6$ and 7. We find that they spin down as a result of gravitational-wave emission and subsequently settle to a stable stationary BH of a spin smaller than $q_{\rm crit}$. For more rapidly spinning unstable BHs, the time scale, for which the new state is reached, is shorter and fraction of the spin-down is larger. Our findings imply that a highly rapidly spinning BH with $q > q_{\rm crit}$ cannot be a stationary product in the particle accelerators, even if it would be formed as a consequence of a TeV-gravity hypothesis. Its implications for the phenomenology of a mini BH are discussed.

DOI: 10.1103/PhysRevD.81.104035 PACS numbers: 04.25.D−, 04.30.−w, 04.40.Dg

I. INTRODUCTION

Clarifying formation and evolution processes of mini black hole (BH) in higher-dimensional spacetimes has become an important issue since a possibility of BH formation in huge particle accelerators was pointed out. If our space is a 3-brane in a higher-dimensional flat spacetime of spacetime dimensionality $d \geq 6$ [1] or in an anti–de Sitter (AdS) spacetime of $d \geq 5$ [2], the Planck energy could be of O(TeV) that may be accessible with particle accelerators in operation, the CERN Large Hadron Collider (LHC). In the presence of the extra dimensions, BHs of very small mass energy $\gtrsim$ TeV may be produced during the particle collision in the accelerators because the true Planck energy may be as low as TeV scale.

A hypothetical phenomenology of a BH produced in the huge particle accelerator was first discussed in [3,4] (see [5] for reviews). According to this standard scenario, a mini BH evolves in the following manner: During the high-energy particle collision of a sufficiently small impact parameter and of energy sufficiently higher than the Planck energy, two particles will merge to form a deformed BH, and then, it settles to a quasistationary state after emission of gravitational waves. The typically assumed time scale for gravitational-wave emission is $\sim 10 r_+/c$ (about 10 times of the dynamical time scale) where r_+ and c are the horizon radius and speed of light, respectively. The quasistationary BH will be subsequently evaporated by the Hawking radiation [6], because of quantum-field-effects in a curved spacetime. Much effort has been devoted to calculating the greybody factor in the Hawking radiation for improving the prediction of signals in the particle-collision experiments [7–12] (see also [13] for related issues).

By contrast, the analyses for BH formation after the particle collision and subsequent evolution by gravitational radiation reaction in higher-dimensional spacetime have not been done yet [but see [14–17] for studies in the four-dimensional (4D) case]. These phases are expected to be described well in the context of general relativity [18], but due to its highly nonlinear nature, any approximation breaks down. Obviously, numerical-relativity simulation is the unique approach for studying this phase.

One of the important issues has been to clarify what type of BH is formed and whether it is stable or not. In the 4D case, any stationary BH formed in vacuum has to be a Kerr BH (neglecting the electric charge of the BH) because of the uniqueness theorem (e.g., [19] for review), and the Kerr BH has been proven to be stable [20–22] (but see [23] for remaining issues for a perfect proof). These facts strongly constrain the possible scenario for mini BH formation and its subsequent evolution. By contrast, there is no uniqueness theorem and no proof for the stability of higher-dimensional BHs (but see [24] for uniqueness of 5D BHs of the spherical horizon topology). As a result, the standard scenario described above (i.e., formation, evolution by subsequent gravitational-wave emission, and evaporation by the Hawking radiation) is quite uncertain.

A mini BH, if it is formed as a result particle collision in a higher-dimensional spacetime, will have only one spin parameter associated with the orbital motion. This can restrict the possibility for the type of the formed BH.

However, even in this case, one cannot restrict the BH type in higher dimensions. For example, in the 5D case, there are many types of BHs: e.g., usual *Kerr-type* BH (Myers-Perry BH [25]) for which surface of the event horizon is S^3, fat and thin *black rings* for which surface has a ringlike shape [26]. Recently, black di-ring [27] and black-saturn [28] solutions were derived as well (see also [29] for other exact solutions of 5D black objects but with two spin parameters). Several authors [8,30,31] discuss a possibility of the black-ring formation in particle collisions. Although it is still an open question, the analysis of apparent horizons in [30] indicates that black-ring formation is not very likely in two point-particle system.

Higher-dimensional BHs with a high spin parameter are known to be unstable against *axisymmetric* perturbations. Emparan and Myers [32] speculated that rapidly spinning BHs with the spacetime dimensionality $d \geq 6$ are subject to the Gregory-Laflamme instability [33], because they have a high degree of ellipticity (i.e., the black membrane limit). Very recently, Dias *et al.* and Murata *et al.* indeed showed, by a linear perturbation analysis, that rapidly spinning BHs for $6 \leq d \leq 9$ are unstable against axisymmetric multiple-ring-like deformation [34,35] (see also related papers [36]).

On the other hand, little is known for the stability of spinning BHs against *nonaxisymmetric* perturbations. Emparan and Myers [32] also speculated, based on a thermodynamic argument, that rapidly spinning BHs with a sufficiently high spin may be unstable against nonaxisymmetric perturbation for $d \geq 5$, because the horizon area (the so-called entropy) of a rapidly spinning BH is often smaller than that of two boosted Schwarzschild BHs with the same total energy and angular momentum. However, the correspondence between the thermodynamical and dynamical instabilities has not been well established. Authors in [37] guess, based on a hydrodynamic/gravity correspondence argument, that a nonaxisymmetric instability may occur for spinning BHs with spin smaller than the critical value for the onset of axisymmetric instabilities. However, a rigorous and quantitative analysis is absent in these studies. To strictly clarify what the criterion for the onset of nonaxisymmetric instabilities is and how the instabilities occur and proceed, we have to solve Einstein's equation. Recently, we performed a numerical-relativity simulation for 5D spinning BHs for the first time, and found that BHs spinning rapidly are dynamically unstable against nonaxisymmetric bar-mode deformation if the spin parameter satisfies the condition $q := a/\mu^{1/2} \gtrsim 0.87$ (see Sec. II for the definitions of q, a, and μ) [38]: An interesting fact is that the critical value we found is close to the value predicted by Emparan and Myers [32], ≈ 0.85, suggesting that their argument relying on BH thermodynamics may be reliable (although we show in this paper that this is not the case for $d \geq 6$).

In this paper, we study the stability of rapidly spinning BHs with dimensionality $d \geq 6$ using a new numerical-relativity code SACRA-ND, which is extended from SACRA [39] and SACRA5D [38]. In this code, Einstein's equation for higher-dimensional spacetimes of any dimensionality for $d \geq 5$ is fully solved without imposing axial symmetry. Thus, in this work, we do not have to assume that the amplitude of the perturbation from the background axisymmetric BH solution is small nor restrict attention to an axisymmetric perturbation. The merits of this approach are that (i) a wide variety of instabilities can be investigated with no ambiguity and with no approximation (except for finite-difference approximation); (ii) the final fate after the onset of the instabilities can be determined because the amplitude of the perturbation from the background BH solution does not have to be small; and (iii) the criterion for the onset of the instabilities is *quantitatively* determined. In this paper, we focus on the six-, seven-, and eight-dimensional (6D, 7D, and 8D) BHs of single spin parameter because such a class of BH is a possible outcome in the particle accelerators. We shall show, for the first time, that the rapidly spinning BHs are dynamically unstable against bar-mode deformation irrespective of the dimensionality. We, furthermore, evolve the 6D and 7D unstable BHs for a long time until they settle to a new stable state. This enables to quantitatively clarify a possible (classical) evolution process of an unstable mini BH for the first time.

The paper is organized as follows. In Sec. II, the formulation for solving Einstein's evolution equation in higher dimensions is described. In Sec. III, a method for evolving Einstein's equation in the spacetime of a special symmetry is summarized. In Sec. IV, we present the numerical results focusing on the criterion for the onset of the bar-mode dynamical instability of rapidly spinning BHs and the fate after the onset of the instability. We will show that the rapidly spinning BHs, which have a spin larger than the critical value, are unstable against spontaneous emission of quadrupole gravitational waves. We will also show that all the unstable BHs, considered in this paper, evolve as a result of gravitational radiation reaction, settling to a stable BH of spin smaller than the critical value. In Sec. V, the conditions for the spontaneous gravitational-wave emission and associated spin-down process are clarified. Section VI is devoted to a summary and discussion. In particular, implications of our results for the phenomenology of a mini BH are discussed in detail.

In Secs. I, II, III, IV, V, and VI B, we adopt the units in which $c = 1$. Only in Sec. VI C, the natural units $c = \hbar = 1$, where $\hbar$ is the Planck constant, are adopted. d denotes the spacetime dimension with $n := d - 4$ being the number of the extra dimension, and G_d denotes the d-dimensional gravitational constant. The Cartesian coordinates (x, y, z, w_q) are used for the space coordinates: $x^a = (x, y, z)$ denote the usual three dimensional coordinates, and w_q ($q = 1 - n$) the coordinates of extra dimension. t denotes the time. Indices i, j, k, and l denote the general spatial coordinates.

II. FORMULATION

We consider a vacuum higher-dimensional spacetime of SO($n+1$) symmetry for which the line element is written as

$$ds^2 = -(\alpha^2 - \beta_k\beta^k)dt^2 + 2\beta_k dx^k dt + \gamma_{ab}dx^a dx^b + \gamma_{nn}d\Omega_n^2, \tag{1}$$

where α is the lapse function, β^k the shift vector, γ_{ij} the space metric, and $d\Omega_n^2$ the line element of n-dimensional unit sphere. γ_{nn} is a conformal factor for the extra-dimensional metric components. x^a denotes (x, y, ρ) where ρ is a radial coordinate

$$\rho = \sqrt{z^2 + \sum_{q=1}^{n} w_q^2}. \tag{2}$$

The geometric quantities in this symmetric spacetime depend only on t, x, y, and ρ. (Note that by SO($n+1$) symmetry, we imply that the subspace of $(z, w_1, \cdots, w_n)$ coordinate directions is isotropic.)

The line element of a Myers-Perry BH of single spin (i.e., the Kerr-type BH) in the Boyer-Lindquist-type coordinates is [25]

$$ds^2 = -d\hat{t}^2 + \frac{\mu}{\hat{r}^{d-5}\Sigma}(d\hat{t} - a\sin^2\theta d\varphi)^2 + \frac{\Sigma}{\Delta}d\hat{r}^2 + \Sigma d\theta^2 + (\hat{r}^2 + a^2)\sin^2\theta d\varphi^2 + \hat{r}^2\cos^2\theta d\Omega_n^2, \tag{3}$$

where μ and a are mass and spin parameters, respectively, $\Sigma := \hat{r}^2 + a^2\cos^2\theta$, and $\Delta := \hat{r}^2 + a^2 - \mu\hat{r}^{5-d}$. Note that the mass and angular momentum of this BH are

$$M = \frac{(d-2)\Omega_{d-2}\mu}{16\pi G_d}, \tag{4}$$

$$J = \frac{2}{d-2}Ma, \tag{5}$$

where Ω_{d-2} is the area of $(d-2)$-dimensional unit sphere, i.e., $\Omega_{d-2} = 2\pi^{(d-1)/2}/\Gamma[(d-1)/2]$. Thus, the line element denoted by Eq. (1) includes the spinning BH solution (3), and nonstationary, nonaxisymmetric deformed states can be described as well.

In numerical simulation, we adopt the Cartesian coordinates (x, y, z, w_q) instead of the curvilinear coordinates; e.g., for $d = 7$, the relations between (z, w_1, w_2, w_3) and radial and angular coordinates $(\rho, \psi, \varphi_1, \varphi_2)$ are

$$z = \rho\cos\psi, \tag{6}$$

$$w_1 = \rho\sin\psi\cos\varphi_1, \tag{7}$$

$$w_2 = \rho\sin\psi\sin\varphi_1\cos\varphi_2, \tag{8}$$

$$w_3 = \rho\sin\psi\sin\varphi_1\sin\varphi_2. \tag{9}$$

Then, Einstein's evolution equation is solved in the Cartesian coordinates using the so-called cartoon method [40,41]. Namely, we solve the equations in the (x, y, z) hyperplane; the hyperplane of $\psi = \varphi_i = 0$. The method used in the present work will be described in the next section.

To solve Einstein's evolution equation in the Cartesian coordinates, we adopt a multidimensional version of the Baumgarte-Shapiro-Shibata-Nakamura (BSSN) formalism [40,42] (see also [43] for a different formalism). We rewrite the line element in the form,

$$ds^2 = -(\alpha^2 - \beta_k\beta^k)dt^2 + 2\beta_k dx^k dt + \chi^{-1}\tilde{\gamma}_{ij}dx^i dx^j, \tag{10}$$

where $\chi = [\det(\gamma_{ij})]^{-1/(d-1)}$ is a conformal factor and the conformal spatial metric $\tilde{\gamma}_{ij}$ satisfies the condition $\det(\tilde{\gamma}_{ij}) = 1$. In addition, we define the following quantities from the extrinsic curvature K_{ij},

$$\tilde{A}_{ij} := \chi\left(K_{ij} - \frac{1}{d-1}\gamma_{ij}K\right), \tag{11}$$

$$K := K_{ij}\gamma^{ij}, \tag{12}$$

as well as an auxiliary variable

$$\tilde{\Gamma}^i := -\partial_j\tilde{\gamma}^{ij}. \tag{13}$$

Then, the variables $(\chi, \tilde{\gamma}_{ij}, K, \tilde{A}_{ij}, \tilde{\Gamma}^i)$ are evolved solving the following equations [40]:

$$(\partial_t - \beta^k\partial_k)\chi = \frac{2}{d-1}\chi(\alpha K - \partial_i\beta^i), \tag{14}$$

$$(\partial_t - \beta^k\partial_k)\tilde{\gamma}_{ij} = -2\alpha\tilde{A}_{ij} + \tilde{\gamma}_{ik}\partial_j\beta^k + \tilde{\gamma}_{jk}\partial_i\beta^k - \frac{2}{d-1}\tilde{\gamma}_{ij}\partial_k\beta^k, \tag{15}$$

$$(\partial_t - \beta^k\partial_k)K = -D_iD^i\alpha + \alpha\left(\tilde{A}^{ij}\tilde{A}_{ij} + \frac{K^2}{d-1}\right), \tag{16}$$

$$(\partial_t - \beta^k\partial_k)\tilde{A}_{ij} = \chi[-(D_iD_j\alpha)^{\mathrm{TF}} + \alpha R_{ij}^{\mathrm{TF}}] + \alpha(K\tilde{A}_{ij} - 2\tilde{A}_{ik}\tilde{A}_j^k) + \tilde{A}_{ik}\partial_j\beta^k + \tilde{A}_{kj}\partial_i\beta^k - \frac{2}{d-1}\tilde{A}_{ij}\partial_k\beta^k, \tag{17}$$

$$(\partial_t - \beta^k\partial_k)\tilde{\Gamma}^i = -2\tilde{A}^{ij}\partial_j\alpha - \tilde{\Gamma}^j\partial_j\beta^i + \frac{2}{d-1}\tilde{\Gamma}^i\partial_j\beta^j + \frac{d-3}{d-1}\tilde{\gamma}^{ik}\partial_k\partial_j\beta^j + \tilde{\gamma}^{jk}\partial_j\partial_k\beta^i + 2\alpha\left[\tilde{\Gamma}^i_{jk}\tilde{A}^{jk} - \frac{d-2}{d-1}\tilde{\gamma}^{ij}\partial_j K - \frac{(d-1)}{2}\frac{\partial_j\chi}{\chi}\tilde{A}^{ij}\right]. \tag{18}$$

Here, D_i and R_{ij} denote the covariant derivative and the Ricci tensor with respect to γ_{ij}, and TF denotes taking the trace-free part.

For evaluating $R^{\rm TF}_{ij}$, we first decompose R_{ij} as

$$R_{ij} = \tilde{R}_{ij} + R^{\chi}_{ij}, \tag{19}$$

where $\tilde{R}_{ij}$ is the Ricci tensor with respect to $\tilde{\gamma}_{ij}$ and we write it in the following form

$$\begin{aligned}\tilde{R}_{ij} =& -\tfrac{1}{2}\tilde{\gamma}^{kl}\tilde{\gamma}_{ij,kl} + \tfrac{1}{2}(\tilde{\gamma}_{ki}\partial_j\tilde{\Gamma}^k + \tilde{\gamma}_{kj}\partial_i\tilde{\Gamma}^k) \\ & - \tfrac{1}{2}[(\partial_l\tilde{\gamma}_{ik})\partial_j\tilde{\gamma}^{kl} + (\partial_l\tilde{\gamma}_{jk})\partial_i\tilde{\gamma}^{kl} - \tilde{\Gamma}^l\partial_l\tilde{\gamma}_{ij}] \\ & - \tilde{\Gamma}^l_{ik}\tilde{\Gamma}^k_{jl}.\end{aligned} \tag{20}$$

Here, $\tilde{\Gamma}^i_{jk}$ is the Christoffel symbol with respect to $\tilde{\gamma}_{ij}$. R^{χ}_{ij} is sum of the terms associated with χ,

$$\begin{aligned}R^{\chi}_{ij} =& \frac{(d-3)}{2\chi}\tilde{D}_i\tilde{D}_j\chi - \frac{(d-3)}{4}\frac{(\tilde{D}_i\chi)\tilde{D}_j\chi}{\chi^2} \\ & + \tilde{\gamma}_{ij}\left[\frac{1}{2\chi}\tilde{D}_k\tilde{D}^k\chi - \frac{d-1}{4\chi^2}(\tilde{D}_k\chi)\tilde{D}^k\chi\right].\end{aligned} \tag{21}$$

Then, we obtain

$$\begin{aligned}R^{\rm TF}_{ij} =& \tilde{R}_{ij} - \frac{1}{d-1}\tilde{\gamma}_{ij}\tilde{\gamma}^{kl}\tilde{R}_{kl} \\ & + \frac{d-3}{2\chi}\left[\tilde{D}_i\tilde{D}_j\chi - \frac{1}{d-1}\tilde{\gamma}_{ij}\tilde{D}_k\tilde{D}^k\chi\right] \\ & - \frac{d-3}{4\chi^2}\left[(\tilde{D}_i\chi)\tilde{D}_j\chi - \frac{1}{d-1}\tilde{\gamma}_{ij}(\tilde{D}_k\chi)\tilde{D}^k\chi\right].\end{aligned} \tag{22}$$

For the 4D case, the so-called puncture gauge conditions are known to be robust for evolving BH spacetime with the BSSN formalism [44]. This is also the case for the higher-dimensional spacetime [40]. However, the freely chosen coefficients in this gauge have to be carefully determined for the stable and long-term evolution. Specifically, we choose the equations in the form

$$\partial_t\alpha = -1.5\alpha K, \tag{23}$$

$$\partial_t\beta^i = 0.3B^i, \tag{24}$$

$$\partial_t B^i = (\partial_t - \beta^k\partial_k)\tilde{\Gamma}^i - \eta_B\mu^{-1/(d-3)}B^i, \tag{25}$$

or

$$\partial_t B^i = \partial_t\tilde{\Gamma}^i - \eta_B\mu^{-1/(d-3)}B^i, \tag{26}$$

where B^i is an auxiliary function, and η_B is a nondimensional constant for which we give different values for different number of d because a small value of η_B is not allowed for a high number of d or for a high spin for achieving the long-term stable numerical evolution. For $d = 5$, we gave $\eta_B = 1$ in the previous work [38]. In the present work, we employ $\eta_B = 2$–5 for $d = 6$, 3–5 for $d = 7$, and 8 for $d = 8$. For unstable BHs, a large value of η_B is favored in performing a long-term simulation until the growth of the instability saturates and subsequently the deformation damps. We tried to use both Eqs. (25) and (26), and found that both of them work well as far as BH spin is not extremely large. For a very high spin ($q \gtrsim 1$), however, Eq. (26) works better than Eq. (25) for a long-term stable simulation.

III. MODIFIED CARTOON METHOD

We solve Einstein's evolution equation in the spacetime of SO($n+1$) symmetry with $n = d-4$ using the Cartesian coordinates $(x, y, z, w_1, \cdots, w_n)$ with the BSSN formalism. The SO($n+1$) symmetry is imposed for the $(z, w_1, \cdots, w_n)$ subspace [i.e., the subspace of $(z, w_1, \cdots, w_n)$ coordinate directions is assumed to be isotropic]. The method is qualitatively the same as those described for 5D spacetime [40]. Namely, we solve the equations in the (x, y, z) hyperplane (i.e., $w_1 = w_2 = \cdots = w_n = 0$ hyperplane), and derivatives with respect to these coordinates are evaluated by a straightforward finite differencing. On the other hand, the derivatives with respect to the extra-dimensional coordinates, w_q ($q = 1 \cdots n$), are evaluated using symmetry relations. In the previous paper [40], we adopted the original prescription in the cartoon method often employed for axisymmetric spacetimes [41]: We prepare 4 additional grid points for the fifth coordinate, w, i.e., $2 \pm \Delta w$ and $\pm\Delta w$. Then, the values for all the geometric quantities at these grid points are determined using the symmetry relation associated with the Killing vector $\partial/\partial\psi$ where $\psi = \tan^{-1}(w/z)$, and then, the derivatives with respect to w are evaluated using a fourth-order finite differencing.

This original method is quite simple for code implementation. However, it is memory-consuming in higher-dimensional simulations, because we have to increase the grid number by a factor of 5 whenever the number of extra dimensions is increased. To save the memory used in computation, we employ a different method in which the derivatives with respect to w_q are replaced to those with respect to z without preparing additional grid points for the extra-dimensional direction. In the following, we describe the new method denoting the scalar, vector, and tensor by Q, Q^i, and Q_{ij}, respectively, and decomposing the subscripts i, j into a, $b = x, y, z$ and w_q ($q = 1-n$).

In the (x, y, z) hyperplane, the following relations hold because of the assumed isotropy:

$$Q_{ww} := Q_{w_1w_1} = \cdots = Q_{w_nw_n} \tag{27}$$

and

$$Q^{w_q} = Q_{aw_q} = Q_{w_qw_r} = 0 \qquad (q \neq r). \tag{28}$$

The derivatives with respect to x^a of Eq. (28) are trivially zero. For other derivatives, the following relations hold: For the scalar quantities,

$$Q_{,w_q} = 0, \qquad Q_{,w_q w_r} = (Q_{,z}/z)\delta_{qr}, \tag{29}$$

for the vector quantities,

$$\begin{aligned} Q^a{}_{,w_q} &= Q^a{}_{,bw_q} = Q^{w_p}{}_{,w_q w_r} = 0, \\ Q^{w_q}{}_{,w_r} &= (Q^z/z)\delta_{qr}, \qquad Q^{w_q}{}_{,w_r a} = (Q^z/z)_{,a}\delta_{qr}, \\ Q^A{}_{,w_q w_r} &= (Q^A{}_{,z}/z)\delta_{qr}, \qquad Q^z{}_{,w_q w_r} = (Q^z/z)_{,z}\delta_{qr}, \end{aligned} \tag{30}$$

and for the tensor quantities,

$$\begin{aligned} Q_{ab,w_q} &= Q_{w_p w_q, w_r} = 0, \qquad Q_{Aw_q,w_r} = (Q_{Az}/z)\delta_{qr}, \\ Q_{zw_q,w_r} &= [(Q_{zz} - Q_{ww})/z]\delta_{qr}, \\ Q_{AB,w_q w_q} &= Q_{AB,z}/z, \qquad Q_{Az,w_q w_q} = (Q_{Az}/z)_{,z}, \\ Q_{zz,w_q w_q} &= Q_{zz,z}/z - (2/z^2)(Q_{zz} - Q_{ww}), \\ Q_{w_q w_q, w_q w_q} &= Q_{ww,z}/z + (2/z^2)(Q_{zz} - Q_{ww}), \\ Q_{w_q w_q, w_r w_r} &= Q_{ww,z}/z \qquad (q \neq r). \end{aligned} \tag{31}$$

Here, A, $B = x$ or y (not z) and δ_{qr} is the Kronecker's delta. We did not evaluate Q_{ij,aw_q} and $Q_{ij,w_q w_r}$ $(q \neq r)$ even if they are not vanishing, because they do not appear in the BSSN equations with SO$(n+1)$ symmetry: Note that the second derivatives appear only in the term $-(1/2)\tilde{\gamma}^{kl}\partial_k\partial_l\tilde{\gamma}_{ij}$ of Eq. (20) and $\tilde{\gamma}^{kl}$ satisfies the relation of Eq. (28). We also do not have to evaluate $Q_{aw_q,ij}$ and $Q_{w_q w_r,ij}$ $(q \neq r)$, because they appear only in the aw_q and $w_q w_r$ components of Eq. (17) with Eq. (20) which do not have to be evolved, as mentioned later.

Some of the above prescriptions can be used only for $z \neq 0$ in computer because of the presence of the terms associated with $1/z$, although these terms are actually regular. Thus for $z = 0$, the following relations, which are found from SO$(n+1)$ symmetry, are employed:

$$\begin{aligned} Q_{,w_q w_q} &= Q_{,zz}, \qquad Q^{w_q}{}_{,w_q} = Q^z{}_{,z}, \qquad Q^A{}_{,w_q w_q} = Q^A{}_{,zz}, \\ Q^z{}_{,w_q w_q} &= 0, \qquad Q_{AB,w_q w_q} = Q_{AB,zz}, \qquad Q_{Az,w_q w_q} = 0, \\ Q_{Aw_q,w_q} &= Q_{Az,z}, \qquad Q_{zw_q,w_q} = 0, \qquad Q_{zz,w_q w_q} = Q_{ww,zz}, \\ Q_{w_q w_q, w_q w_q} &= Q_{zz,zz}, \qquad Q_{w_q w_q, w_r w_r} = Q_{w_q w_q, zz}. \end{aligned} \tag{32}$$

The final remark is on the treatment of the advection terms such as $\beta^k\partial_k\tilde{\gamma}_{ij}$: Because $\beta^{w_q} = 0$ for the $w_q = 0$ hyperplane in the present case, the advection terms associated with β^{w_q} is always vanishing in the computational domain chosen in our method.

With these prescriptions, all the derivatives associated with the extra-dimensional coordinates can be replaced to the finite-differencing terms with respect to x^a or with no finite differencing. It is worthy to note that total amount of computational operation is only slightly larger than that for the $3+1$ case.

Because of the relations (27) and (28) that follow from SO$(n+1)$ symmetry, the implementation for the higher-dimensional contribution can be even simplified: We have only to evolve the scalar equations, the "a" components of the vector equations, and the "ab" components and (one of) the $w_q w_q$ components of the tensor equations (i.e., the equations for $\tilde{\gamma}_{ij}$ and $\tilde{A}_{ij}$) of the BSSN formalism. Therefore, we need to increase only one component for $\tilde{\gamma}_{ij}$ and $\tilde{A}_{ij}$ irrespective of the dimensionality. In the evolution equation, we often have terms such as $\beta^i{}_{,i}$ or $\tilde{\gamma}^{kl}\tilde{\gamma}_{ak,l}$, which are evaluated by

$$\beta^i{}_{,i} = \beta^a{}_{,a} + n\beta^{w_1}{}_{,w_1}, \tag{33}$$

$$\tilde{\gamma}^{kl}\tilde{\gamma}_{ak,l} = \tilde{\gamma}^{cd}\tilde{\gamma}_{ac,d} + n\tilde{\gamma}^{w_1 w_1}\tilde{\gamma}_{aw_1,w_1}, \tag{34}$$

where the prescriptions shown in Eqs. (29)–(32) are used for evaluating the second terms in the right-hand side. These facts imply that once a 5D code is implemented, it is quite straightforward to extend it to a code for $d \geq 6$, even when we do not employ a curvilinear coordinate system [43].

IV. NUMERICAL SIMULATION

A. Setting and methodology

We prepare 6D–8D Myers-Perry BHs of single spin parameter [see Eq. (3) for the line element in the Boyer-Lindquist coordinates] as the initial condition. Because the Boyer-Lindquist coordinates are not suitable for the Cauchy evolution of BH spacetimes, we transform the radial coordinate introducing a quasiradial coordinate r; we rewrite the line element in the form (see [45] for the 4D case)

$$\begin{aligned} ds^2 = &-dt^2 + \frac{\mu}{\hat{r}^{d-5}\Sigma}(dt - a\sin^2\theta d\varphi)^2 + \Phi(dr^2 + r^2 d\theta^2) \\ &+ (\hat{r}^2 + a^2)\sin^2\theta d\varphi^2 + \hat{r}^2\cos^2\theta d\Omega_n^2, \end{aligned} \tag{35}$$

where Φ is a conformal factor for the (r, θ) plane. Namely, the two-dimensional metric for (r, θ) is written in a conformally flat form, and the following relations are satisfied:

$$\Phi^{1/2} dr = \pm(\Sigma/\Delta)^{1/2} d\hat{r}, \tag{36}$$

$$\Phi^{1/2} r = \Sigma^{1/2}. \tag{37}$$

Then, r is defined by

$$r = r_h \exp\left[\pm \int_{r_+}^{\hat{r}} \frac{dR}{\sqrt{R^2 + a^2 - \mu R^{5-d}}}\right], \tag{38}$$

where the plus and minus signs are adopted for the regions $r \geq r_h$ and $r \leq r_h$, respectively. r_+ is the horizon radius in the Boyer-Lindquist coordinates and a positive root of $r_+^2 + a^2 = \mu r_+^{5-d}$. r_h is the horizon radius in the quasiradial coordinate, which is determined by the condition $r = \hat{r}$ for $\hat{r} \to \infty$. A fourth-order numerical integration is per-

formed for the integral of Eq. (38) using the Bode's rule [46] because it cannot be analytically integrated in general.

With this transformation, the $t = \text{const}$ hypersurface becomes spacelike everywhere for $0 \le r < \infty$, and furthermore, the singularity, which is originally located at $\hat{r} = 0$, is excluded. More specifically, the spacelike hypersurface has an inversion symmetry with respect to $r = r_h$ hypersphere (i.e., this hypersphere is the wormhole throat), and thus the "point," $r = 0$, represents the spacelike infinity of (say) another world beyond the horizon. Although this point is not a physical singularity, it becomes a coordinate singularity, because Φ is proportional to r^{-4} irrespective of the number of d. However, the puncture approach [specifically, appropriate choice of the conformal factor in numerical simulation, $\chi = [\det(\gamma_{ij})]^{-1/(d-1)}$, and choice of the puncture gauge (23)–(25)] enables to stably evolve a BH spacetime with no difficulty [40,44].

The condition for the onset of instabilities for spinning BHs depends on a nondimensional spin parameter. Because the stability does not depend on the magnitude of μ, all dimensional quantities can be scaled out of the problem appropriately normalizing them by using μ: Specifically, $\mu^{1/(d-3)}$ has the dimension of length and time in the $c = 1$ units (and is often referred to as r_s, e.g., [10]), and thus, we should define a nondimensional spin as

$$q := \frac{a}{\mu^{1/(d-3)}}. \tag{39}$$

The stability of a Myers-Perry BH depends only on this quantity. Note that this is different from $a_* := q/r_+$ which is often used as another nondimensional spin parameter [4,10].

Numerical simulation is performed in the (x, y, z) coordinates, and thus, the initial condition is prepared by performing a coordinate transformation from (r, θ, φ) to (x, y, z). In addition, we add a small bar-mode perturbation to the conformal factor χ as

$$\chi = \chi_0\left[1 + A\frac{x^2 - y^2}{\mu^{2/(d-3)}}\exp\left(-\frac{r^2}{2r_h^2}\right)\right], \tag{40}$$

where χ_0 is the nonperturbed solution and A the initial perturbation amplitude, $A \ll 1$. We focus here on the bar mode because it is often the most relevant unstable mode for self-gravitating, dynamically unstable rotating systems such as a rotating star [47]. We chose the value of A for a wide range from 10^{-6} to 0.02 and found that for unstable BHs, the growth rate of the unstable mode does not depend on the initial magnitude of A. Taking into account this result, in a long-term evolution of unstable BHs for studying the nonlinear growth of the unstable mode, we choose a relatively large value of $A = 0.005$ or 0.02 to save computational costs. It should be also pointed out that the numerical error accumulates with time and a significant resolution is needed to suppress it. This implies that if a simulation was started with a very small value of A, quite expensive computational costs would be required to accurately follow the nonlinear growth of the perturbation.

Initially, the lapse function is chosen as $\alpha = \chi$. With this modification, α becomes positive except for $r = 0$ where $\alpha = 0$ (near $r = 0$, α is proportional to r^4 with this choice). On the other hand, the shift vector is not modified; we choose the same shift as in the Myers-Perry BH initially.

We solve Einstein's evolution equation in the BSSN formalism using a new code, SACRA-ND, in which an adaptive mesh refinement (AMR) algorithm is implemented in the same manner as in SACRA [39]. Because we solve the higher-dimensional equations only with the (x, y, z) coordinates, the methods of interpolation, extrapolation, and evolution for the grid structure in SACRA-ND are totally the same as those in SACRA: All the spatial derivatives with respect to $x^a = (x, y, z)$ are evaluated using a centered fourth-order finite differencing except for the advection term such as $\beta^k \partial_k \chi$ for which a fourth-order upwind scheme is adopted. The time evolution is carried out using the standard fourth-order Runge-Kutta method [46]. The reader may refer to [39] for details about the numerical methods.

For the AMR scheme, we prepare 6 refinement levels in the present numerical simulation. As a test, we performed several simulations enlarging the computational domain with 7 refinement levels while the grid resolution in the finest level is unchanged. We found that the results shown in Sec. IV are essentially independent of the location of the outer boundary. Computational domain for each refinement level has a half cubic shape which covers $[-L_l{:}L_l]$ for x and y, and $[0{:}L_l]$ for z; we assume the equatorial plane symmetry. Here, L_l denotes the location of the refinement boundary for the lth refinement level with $l = 0$–N_l and $N_l = 5$ in the present work. We note that in SACRA and SACRA-ND, six grid points are prepared outside the refinement boundaries for buffer zone in each refinement level, following [48]. The relation $L_l = 2L_{l+1}$ is imposed for SACRA-ND. Irrespective of l, we assign $2N + 1$ vertex-centered grid points for $[-L_l{:}L_l]$ where N was chosen to be 30, 40, and 50 for checking convergence: We monitored the violation of the Hamiltonian and momentum constraints, conservation of gravitational mass, and conservation of the area and spin of BHs (for stable model), and checked that the convergence with improving the grid resolution is achieved. The grid spacing is L_l/N and L_{N_l} is chosen to be $1.2\mu^{1/(d-3)}$ irrespective of the number of d. For the best resolved run, the apparent horizon radius is covered by 30–40 grid points for rapidly spinning BHs: We note that the initial coordinate radii of the BH horizon, $r_h/\mu^{1/(d-3)}$, are in the range 0.584–0.630 ($q = 1.143 - 0$, minimum at $q \sim 1$) for $d = 6$, $0.750 - 0.707$ ($q = 1.013 - 0$) for $d = 7$, and $0.812 - 0.758$ ($q = 0.832 - 0$) for $d = 8$, respectively. Because of our choice

of the puncture gauge, this coordinate radius increases by a factor of 1.3–1.5 during evolution.

A steep gradient always appears for geometric quantities near the origin for rapidly spinning BHs in the puncture gauge, and this often causes a problem for stably evolving the BHs, although such region is not important for studying the stability of the BH at all. Thus, we employ a very simple excision method for discarding this region. Specifically, for $r \le r_{\rm ex}$, we set $\tilde{\gamma}_{ij} = \delta_{ij}$ and $\tilde{A}_{ij} = K = 0$. Other quantities, α, β^k, χ, and $\tilde{\Gamma}^i$, are solved without any prescription. In this work, $r_{\rm ex}$ is chosen to be $0.3\mu^{1/(d-3)}$ or $0.4\mu^{1/(d-3)}$ which is typically $\sim$30%–40% of the apparent horizon radius; thus, the excised region is well inside the BH horizon. Because no information escapes from the BH horizon and there are many grid points covering the inside of apparent horizon, the results are insensitive to the choice of $r_{\rm ex}$ as far as it is sufficiently small. We note that this method is acceptable for the case that an unstable BH deforms by a moderate degree (for $\eta \lesssim 0.5$; see Sec. IV B for definition of η). For a highly nonlinear deformation, however, we will have to develop other prescriptions for handling the steep gradient near the central region, which is beyond the scope of this paper.

B. Numerical results

1. Critical spin for bar-mode instability

During numerical simulation, we determine the apparent horizon and calculate its area and circumferential radii to investigate the properties of the unstable BHs. We also extract gravitational waves of quadrupole mode in a local wave zone.

To determine the stability of a BH against bar-mode deformation, we monitor two quantities. One is a deformation parameter of the BH horizon. To define this parameter, we first calculate circumferential radii of the apparent horizon along several meridians. Specifically, we measure the proper length of the meridians for $\varphi = 0$ (and π), $\pi/4$ (and $5\pi/4$), $\pi/2$ (and $3\pi/2$), and $3\pi/4$ (and $7\pi/4$); the proper length of each meridian for a given value of $\varphi(<\pi)$ is defined by

$$l_\varphi = 2\int_0^{\pi/2} (\sqrt{\gamma_{\theta\theta}(\varphi)} + \sqrt{\gamma_{\theta\theta}(\varphi+\pi)}) d\theta. \tag{41}$$

Then, we define a bar-mode deformation parameter

$$\eta := \frac{2\sqrt{(l_0 - l_{\pi/2})^2 + (l_{\pi/4} - l_{3\pi/4})^2}}{l_0 + l_{\pi/2}}. \tag{42}$$

The value of η is zero for an axisymmetric apparent horizon, and increases as the deviation from the axial symmetry is enhanced. Thus, η is an indicator of nonaxisymmetric bar-mode deformation. A drawback of the diagnostic with this quantity is that the apparent horizon is a coordinate-dependent notion, and thus, η may not exactly trace the deformation of the BH, although the apparent horizon agrees with the event horizon for a stationary spacetime, and hence, for $\eta \ll 1$, they are likely to agree, at least approximately, with each other.

The other more physical quantity for measuring the deformation of a BH is gravitational waveform observed in a wave zone. This quantity should be coordinate-invariant, and thus, tells us whether the BH spacetime is stable or not with no ambiguity. In this work, we monitor a dimensionless form of gravitational waves

$$h_+ := \frac{\tilde{\gamma}_{xx} - \tilde{\gamma}_{yy}}{2}\left[\frac{r}{\mu^{1/(d-3)}}\right]^{(d-2)/2} \tag{43}$$

$$h_\times := \tilde{\gamma}_{xy}\left[\frac{r}{\mu^{1/(d-3)}}\right]^{(d-2)/2} \tag{44}$$

along the z-axis. Here, r is the coordinate distance from the center, and h_+ and $h_\times$ are regarded as the plus (+) and cross ($\times$) modes of quadrupole gravitational waves in the wave zone.

Figure 1(a) plots the evolution of η for $d = 6$ and for the initial spin $q_i = a_i/\mu^{1/3} = 0.674$–$1.039$ with $A = 0.005$. This shows that for $t/\mu^{1/3} \gtrsim 10$, the value of η increases or decreases in an exponential manner as

$$\eta = \eta_0 e^{t/\tau}, \tag{45}$$

where τ is the growth time scale and η_0 is a constant. Figure 1(b) plots the growth rate, τ^{-1}, in units of $\mu^{-1/3}$ as a function of q_i. We determine τ by the least-square fitting of the curve of $\ln\eta$ with linear lines for $15 \le t/\mu^{1/3} \le 100$ or for the data of $15 \le t/\mu^{1/3}$ and $\eta \le 0.1$. These figures show that for $q_i \gtrsim 0.75$, η grows exponentially with time, and otherwise, it damps exponentially. Therefore, the BHs with $q_i \gtrsim 0.75$ are dynamically unstable against bar-mode deformation [the critical value, $q_{\rm crit}$, is found to be ≈ 0.743 by interpolation; cf. Fig. 1(b)]. Because they are dynamically unstable, such BHs have a quasinormal mode with a negative value of the imaginary part of eigen angular frequency, $\omega_I := {\rm Im}(\omega_{\rm QN})$, and the bar-mode deformation grows in proportional to $e^{i\omega_{\rm QN}t} \propto e^{-\omega_I t}$. On the other hand, the BH with $q_i \lesssim 0.74$ is stable, and thus, ω_I are positive for any mode (strictly speaking, there might exist a mode of $\omega_I < 0$ with $|\omega_I|$ less than $\sim 0.01\mu^{-1/3}$ because we performed the simulations only for a finite duration of order $100\mu^{1/3}$).

Figure 1(b) shows that the growth rate of the instability, τ^{-1}, increases monotonically with the spin q, and approximately linearly in q for $0.74 \le q \lesssim 1$. The growth rate (τ^{-1} or ω_I) is approximately described as $C_\tau(q - q_{\rm crit})$ where C_τ is a constant $\approx 0.51\mu^{-1/3}$.

The growth time scale of the bar-mode deformation for the BHs of spin slightly larger than $q_{\rm crit}$ is of order $100\mu^{1/3}$ (the damping time scale for a stable BH with $q \lesssim q_{\rm crit}$ is also of this order). This is much longer than the spin period

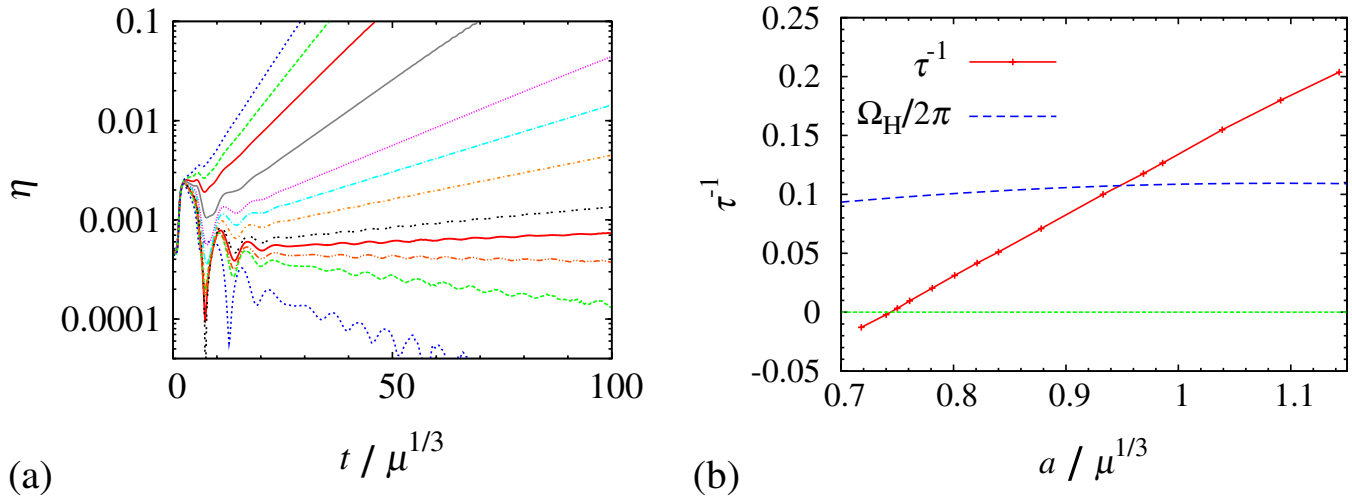

FIG. 1 (color online). (a) Evolution of deformation parameter η for $d = 6$ and for the initial spin $q_i = a/\mu^{1/3} \approx 1.039$, 0.986, 0.933, 0.878, 0.821, 0.801, 0.781, 0.761, 0.750, 0.740, 0.718, and 0.674 (from the upper to lower curves) with $A = 0.005$. (b) The growth rate of η, $1/\tau$, in units of $\mu^{-1/3}$ as a function of q (solid curve). The dashed curve denotes $\Omega_{\rm H}/2\pi$. For $q_i \gtrsim 0.75$, the value of η increases exponentially with time, and otherwise, an exponential damping is seen. For $q_i = 0.750$ (thick solid curve in panel (a)) and 0.740 (below the curve of $q_i = 0.750$), the growth and damping rates of η are quite small, indicating that these BHs are close to the marginally stable state.

of the BHs defined by $2\pi/\Omega_{\rm H} = O(10\mu^{1/3})$ where $\Omega_{\rm H} = a/(r_+^2 + a^2)$ is the angular velocity of the BH horizon. Thus, the instability grows slowly with a time scale much longer than the dynamical time scale $\sim r_+/c$ for $q \sim q_{\rm crit}$. For a much larger value of q, however, the growth time scale is much shorter: We find that τ is as short as $2\pi/\Omega_{\rm H}$ for $q \approx 0.95$, and as $\pi/\Omega_{\rm H}$ for $q \approx 1.15$. Simply extrapolating the approximately linear relation for $\tau^{-1}(q)$, τ is likely to be much shorter than $2\pi/\Omega_{\rm H}$ for $q \gg 1$. Implications of these properties for the evolution of rapidly spinning BHs will be discussed in Secs. V B and VI.

Figure 2(a) plots the long-term evolution of η for $d = 6$ and for $q_i = 0.801$ with several magnitudes of initial perturbation ($A = 10^{-6}$, 0.001, 0.005, and 0.02) and for different grid resolutions ($N = 30$, 40, and 50 for $A = 0.005$, and $N = 40$ and 50 for $A = 0.02$). This shows that the growth rate is independent of the initial perturbation magnitude, implying that the instability sets in irrespective of initial perturbation; even from an infinitesimally small perturbation, the instability grows spontaneously. The growth rate depends weakly on the grid resolution; for a poor grid resolution ($N = 30$), the growth rate is underestimated. However, for $N \geq 40$, it appears to approximately converge, and thus, the simulations with $N \geq 40$ (grid spacing smaller than $0.03\mu^{1/3}$) have an acceptable resolution.

After the value of η reaches the maximum, the growth of the instability terminates, and then, η damps exponentially with time. The reason for this is that during the nonlinear growth of the bar-mode deformation, gravitational-wave emission is enhanced, and energy and angular momentum of the BHs are carried away. As a result, the BH spin parameter, q, *decreases* and at the saturation, it reaches a stable state with $q < q_{\rm crit}$, for which the sign of the imaginary part of eigen angular frequency for the corresponding quasinormal mode changes to be positive. The evolution of the BH spin will be analyzed in detail in Sec. IV B 2. Here, we show an indirect evidence that this interpretation is correct: The saturation value of η is larger for the BHs of larger initial spin, because the required spin-down fraction is $q_i - q_{\rm crit}$. Figure 2(b) plots the evolution of η for $A = 0.02$ and for relatively small initial spins, $q_i = 0.821$, 0.801, and 0.781. Figure 2(c) is the same as Fig. 2(b) but for large initial spins $q_i = 0.878$, 0.933, 0.986, and 1.039 with $A = 0.005$. These clearly illustrate that for the larger initial spin, a BH has to emit more gravitational waves for spinning down to reach a stable BH, and hence, the nonlinear growth of the bar-mode deformation has to continue until a high saturation value of η is reached. Figure 2(d) plots the maximum value of η, $\eta_{\rm max}$, as a function of q_i. This clearly shows that the value of $\eta_{\rm max}$ increases systematically with q_i: The relation between $\eta_{\rm max}$ and q_i is approximately written in the form (68) (see Sec. VI B for an approximate derivation of this relation). This result suggests that for $q_i \gg 1$, the BH may reach a highly deformed state with $\eta \sim 1$ (although we were not able to evolve such ultra spinning BHs in the present work.)

The numerical results obtained in this paper are approximately derived using a semianalytic calculation, as illustrated here. Based on the analytic calculations, we will show in Sec. V that the BH spin should be decreased by gravitational radiation reaction.

It is worthy to note that for the larger initial spin $q_i \sim 1$, the damping time scale for the bar-mode deformation after

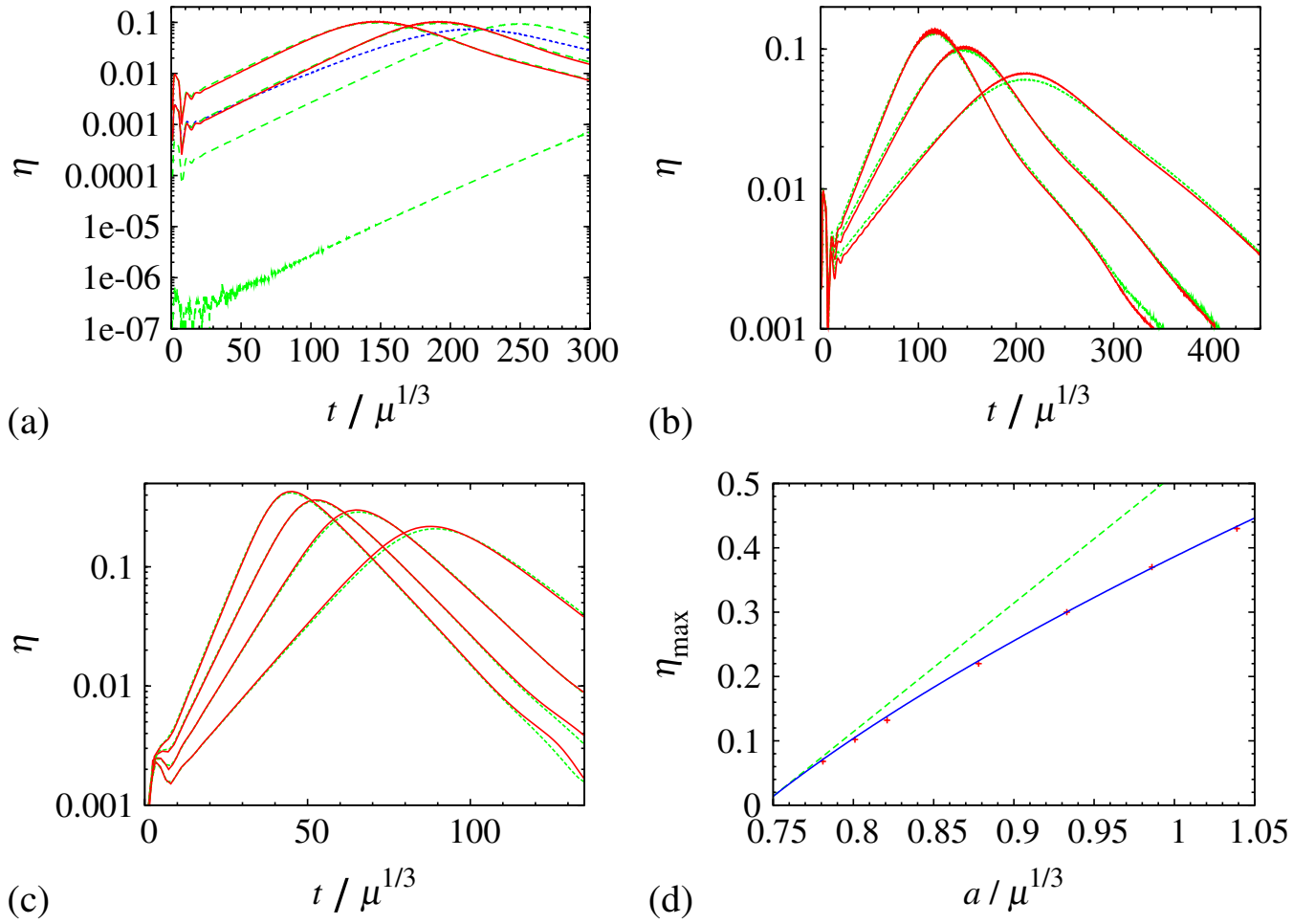

FIG. 2 (color online). (a) Evolution of deformation parameter η for $d = 6$ and for $q_i = 0.801$ with initial perturbation amplitude $A = 0.02$, 0.005, 0.001, and 10^{-6} (from the upper to lower curves) and with $N = 30$ (dotted curve), 40 (dashed curves), and 50 (solid curves), respectively. (b) The same as (a) but for $q_i = 0.821$, 0.801, and 0.780 (from left to right) with $A = 0.02$ and with $N = 40$ (dashed curves) and 50 (solid curves). (c) The same as (b) but for $q_i = 1.039$, 0.986, 0.933, and 0.878 (from the upper to lower curves) with $A = 0.005$. (d) The maximum value of η as a function of q_i. The dashed line and solid curve denote $\eta_{\max} = 2(q_i - q_{\rm crit})$ and relation (68), respectively, (see Sec. VI B for an approximate derivation of these relations).

the saturation is reached depends weakly on the initial spin: The time scale (the duration until $\eta \le 10^{-3}$ is reached) is $\sim 100\mu^{1/3}$. This seems to be due to the fact that the damping time scale depends primarily on the BH state after the saturation is reached; i.e., the property of a BH of spin $q \lesssim q_{\rm crit}$ determines the damping time scale. The damping time duration is fairly long $\sim 100\mu^{1/3}$, implying that the unstable BHs always have to spend a long time until they reach a stationary, stable state.

Figure 3(a) plots the evolution of η for $d = 7$ and $q_i = a/\mu^{1/4} = 0.719$–$0.960$. This shows that for $q_i \gtrsim 0.735$, η grows exponentially with time, and otherwise, it damps exponentially. Figure 3(b) displays the growth rate, τ^{-1}, in units of $\mu^{-1/4}$, and shows that it monotonically increases, approximately linearly with q for $0.719 \le q \lesssim 1$ as in the case of $d = 6$. The critical spin for the onset of the bar-mode instability is determined as $q_{\rm crit} \approx 0.730$, and near $q = q_{\rm crit}$ the growth rate (τ^{-1} and ω_I) behaves as $C_\tau(q - q_{\rm crit})$ where C_τ is a constant $\sim 0.54\mu^{-1/4}$. It is interesting to note that the coefficient $C_\tau \mu^{1/(d-3)}$ for $d = 7$ is close to that for $d = 6$.

The critical spin, $q_{\rm crit}$, for the onset of the bar-mode instability is also very close to that for $d = 6$. Simulations for $d = 8$ also clarified that the critical spin is $q_{\rm crit} \approx 0.77$, where $q = a/\mu^{1/5}$ for $d = 8$, again close to those for $d = 6$ and 7. This suggests that the critical value of q depends weakly on the value of d as long as $d \ge 6$ (note, however, that for $d = 5$, we found it a relatively large value, ≈ 0.87 [38]). The values of $q_{\rm crit}$ and the corresponding values of $a_* = a/r_+$ are summarized in Table I.

As in the case $d = 6$, the growth rate, τ^{-1}, increases monotonically with the value of q_i for $d = 7$. For $q_i \gtrsim 0.92$, it is larger than the BH spin frequency $\Omega_{\rm H}/2\pi$. This indicates the growth time scale is much shorter

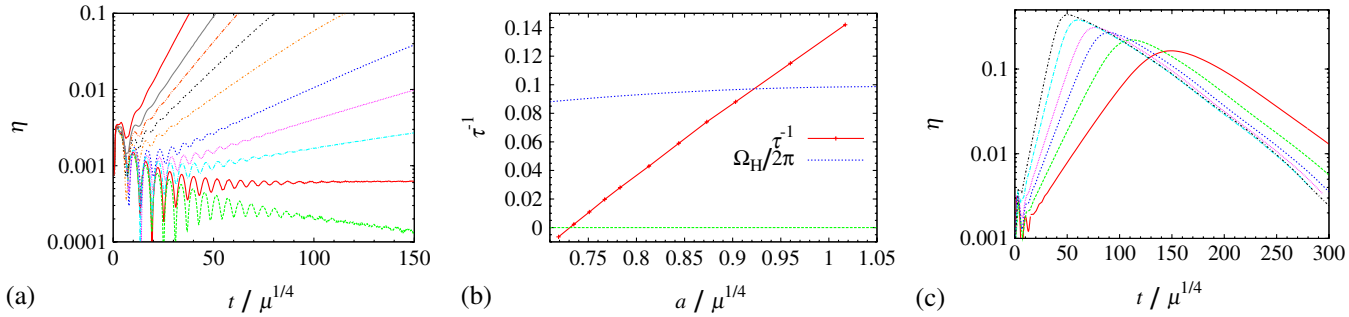

FIG. 3 (color online). (a) The same as Fig. 1 but for $d = 7$ and for $q_i = a/\mu^{1/4} = 0.960$, 0.903, 0.844, 0.813, 0.783, 0.767, 0.751, 0.735, and 0.719 (from the upper to lower curves) with $N = 50$. For $q_i \gtrsim 0.73$, the value of η increases exponentially with time, otherwise, an exponential damping is seen. For $q = 0.735$, the growth (or damping) rate of η is close to zero, implying that this BH is close to the marginally stable one. (b) The growth rate of η, $1/\tau$, in units of $\mu^{-1/4}$ as a function of q (solid curve). The dashed curve denotes $\Omega_{\rm H}/2\pi$. (c) The same as panel (a) but for long runs with $q_i = 1.017$, 0.960, 0.903, 0.873, 0.844, and 0.813.

than the BH spin for $q_i \gg 1$ irrespective of the dimensionality.

Figure 3(c) plots the long-term evolution of η for $d = 7$ with higher spins, $q_i = 0.813$–1.017. For these BHs, the growth of the bar-mode deformation saturates at a large value of η as $\eta_{\rm max} = 0.1$–0.5 due to gravitational radiation reaction, and then, η decreases exponentially as in the case of $d = 6$. At the saturation, the BH spin parameter, q, is likely to be slightly smaller than $q_{\rm crit}$. As in the case of $d = 6$, the damping rate of the bar-mode deformation after the saturation is reached depends only weakly on the initial value of q_i. The reason for this is that it depends primarily on the spin achieved just after the saturation is reached ($q \lesssim q_{\rm crit}$), as mentioned before. One point to be noted is that the damping time-scale is much longer than the growth time-scale for $q_i \sim 1$ (in the 6D case, two time-scales are not very different and smaller than $50\mu^{1/3}$). The damping time-scale is $\gtrsim 100\mu^{1/4}$ in the 7D case. This suggests that it always takes a long time for the unstable BHs to reach a stable state for $d \geq 7$.

To confirm that the bar-mode deformation of the BHs is indeed physical (the growth of η is not due to a coordinate choice for finding apparent horizons), we extract gravitational waves in the wave zone. Figure 4 plots gravitational waveforms, h_+ and $h_\times$, as a function of a retarded time $t - r$ for $d = 6$ and for $q_i \approx 0.801$ and 0.986. We note that gravitational waveforms for different values of q_i are qualitatively similar. Here, r denotes the coordinate distance of extracting gravitational waves. We also plot together evolution of $\eta/2$ as a function of t. As in the behavior of η, the amplitude of gravitational waves increases exponentially with time in the early phase, and after the saturation point is reached, it starts exponential damping. For the larger initial spin, the growth time scale is shorter; for $q_i = 0.986$, the grow time-scale is comparable to the oscillation period. h_+ and $h_\times$ behave essentially in the same manner except for a phase difference of $\pi/2$. The amplitude of gravitational waves is approximately equal to $\eta/2$ for the small amplitude and slightly smaller than $\eta/2$ for the amplitude $(h_+^2 + h_\times^2)^{1/2} \gtrsim 0.1$. This slight disagreement in the amplitude for the high-amplitude case is likely due to the fact that the nonlinear deformation of the BH enhances the amplitude of gravitational waves of modes other than the quadrupole ones, suppressing the quadrupole modes. It is worthy to point out that the oscillation frequency remains approximately constant (besides a small secular shift associated with the evolution of the BHs). This indicates that one fundamental quasinormal mode contributes to the instability.

TABLE I. The values of $q_{\rm crit}$ and the corresponding values of a_* and C_p/C_e for $d = 5$–8. C_p/C_e is defined in Eq. (48).

d	5	6	7	8
$q_{\rm crit}$	0.87	0.74	0.73	0.77
a_*	1.76	0.91	0.83	0.86
C_p/C_e	0.38	0.65	0.68	0.67

2. Evolution of spin and area

Now, we illustrate how the BH spin evolves as a result of gravitational radiation reaction. To approximately determine the value of the BH spin from the shape of apparent horizon, we calculate the ratio of a polar circumferential length, C_p, to the equatorial circumferential length, C_e, for which we define

$$C_p := \frac{l_0 + l_{\pi/2}}{2}, \tag{46}$$

$$C_e := \int_0^{2\pi} \sqrt{\gamma_{\varphi\varphi}} d\varphi, \tag{47}$$

where the integral for C_e is performed along the surface of the apparent horizon at $\theta = \pi/2$. For the Myers-Perry BH of single spin, the ratio C_p/C_e is given by

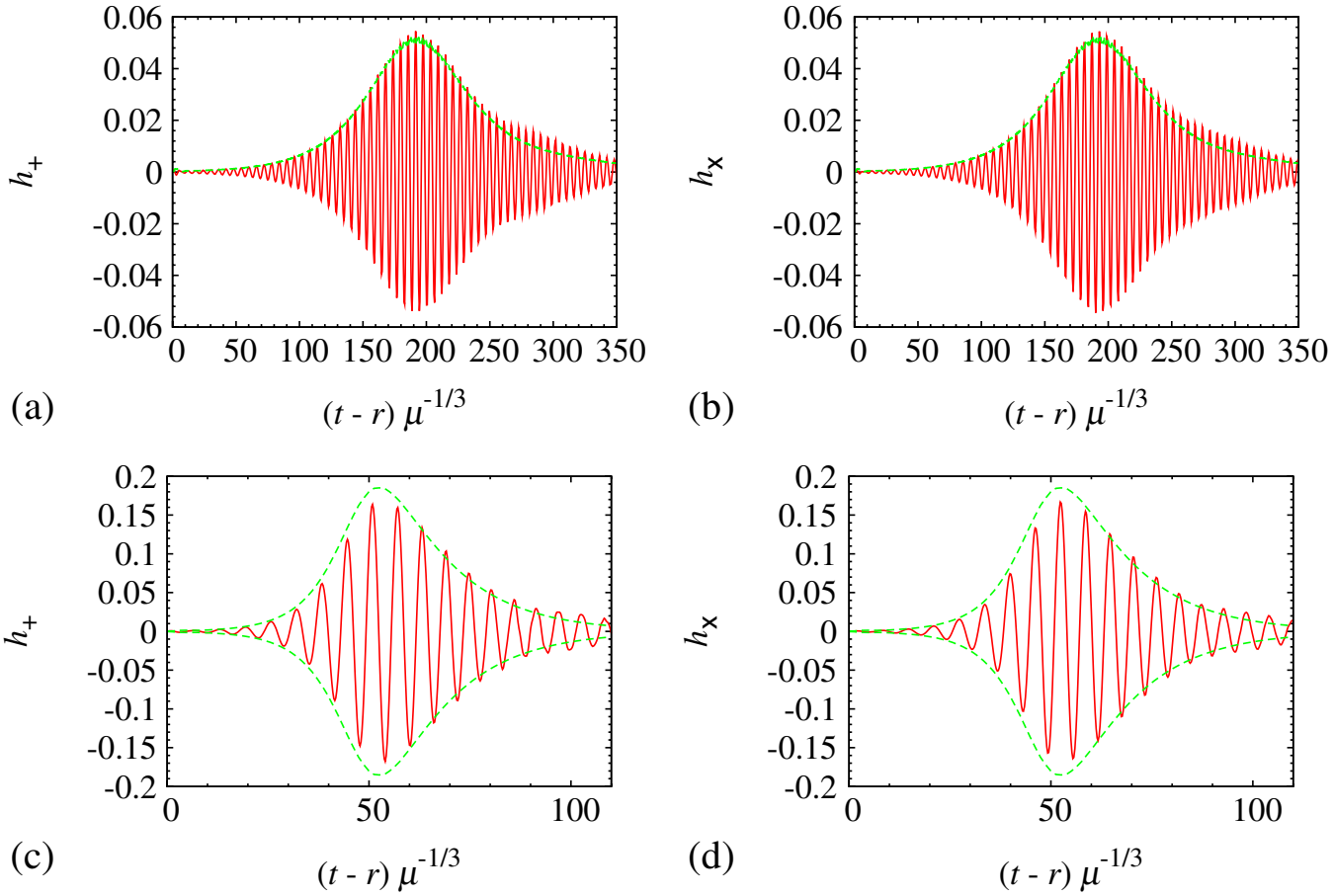

FIG. 4 (color online). (a) and (b): + and × modes of gravitational waveform (solid curve) from an unstable BH for $d = 6$ and for $q_i = 0.801$ as a function of a retarded time defined by $t - r$ where r is the coordinate distance from the center. We also plot $\eta/2$ as a function of t (dashed curve). The initial condition is $A = 0.005$ and the result for the grid resolution of $N = 50$ is plotted. (c) and (d): The same as (a) and (b) but for $d = 6$ and for $q_i = 0.986$ with $A = 0.005$.

$$\frac{C_p}{C_e} = \frac{2r_+^{d-3}}{\pi\mu}\int_0^{\pi/2}\sqrt{1+\frac{a^2\cos^2\theta}{r_+^2}}d\theta, \tag{48}$$

which is a monotonically decreasing function of $q = a/\mu^{1/(d-3)}$ for any given number of d (see Fig. 5). Thus, as far as the state of a BH is close to an axisymmetric stationary BH, we may use it for measuring the spin, q. We note that 5D BHs become dynamically unstable only for a small value of $C_p/C_e \lesssim 0.38$ [38], whereas for $d \geq 6$, the critical values of C_p/C_e are rather large universally; $C_p/C_e = 0.65$ for $d = 6$, 0.68 for $d = 7$, and 0.67 for $d = 8$ (listed in Table I). This illustrates that the 5D BHs are qualitatively different from the higher-dimensional BHs with $d \geq 6$.

Figure 6(a) plots the evolution of C_p/C_e for $d = 6$ and for relatively small initial spins $q_i = 0.821$, 0.801, and 0.781. The initial value of this ratio is ≈ 0.587 for $q_i = 0.821$, ≈ 0.602 for $q_i = 0.801$, and ≈ 0.618 for $q_i = 0.781$, respectively. When η is much smaller than 0.1, the value of C_p/C_e remains approximately constant. With the nonlinear growth of the bar-mode deformation, it starts increasing due to the decrease of the spin by gravitational radiation reaction, and it eventually settles

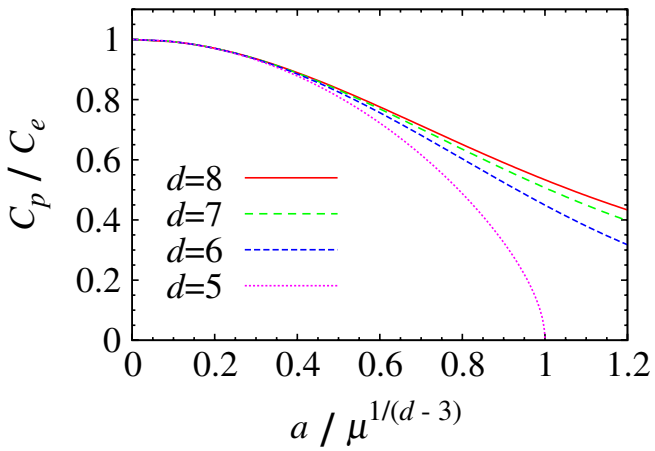

FIG. 5 (color online). C_p/C_e as a function of $q = a/\mu^{1/(d-3)}$ for $d = 5$–8.

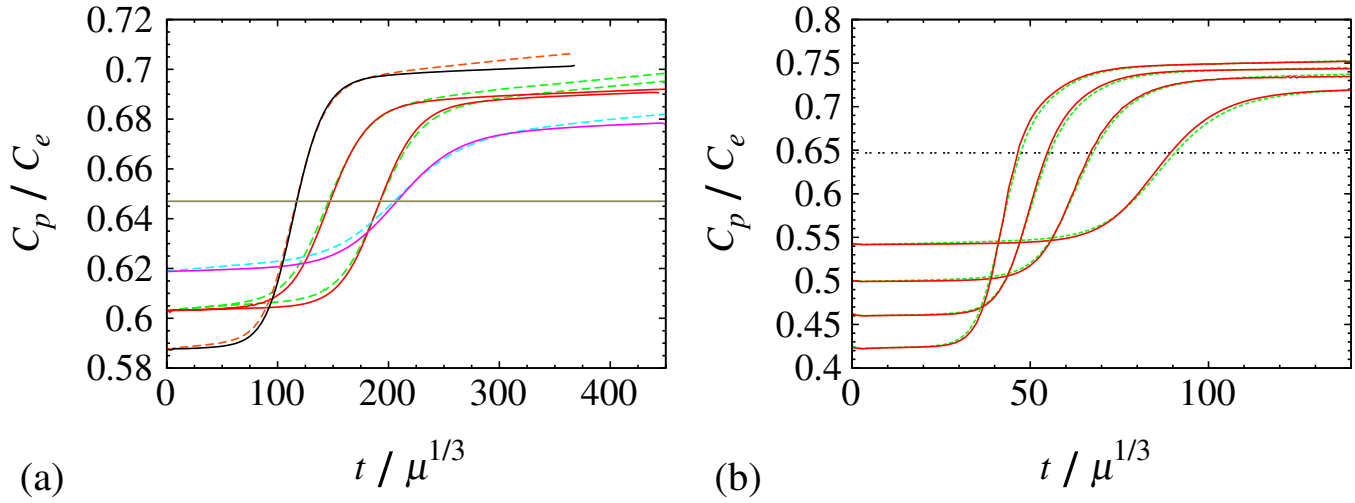

FIG. 6 (color online). (a) Evolution of C_p/C_e for $d = 6$ and for relatively small initial spins $q_i = a/\mu^{1/3} = 0.821$ ($C_p/C_e \approx 0.587$ at $t = 0$), 0.801 ($C_p/C_e \approx 0.602$ at $t = 0$), and 0.781 ($C_p/C_e \approx 0.618$ at $t = 0$) as a function of time. For $q_i = 0.801$, the results with $A = 0.02$ and 0.005 are plotted. For $q_i = 0.821$ and 0.781, the results with $A = 0.02$ are plotted. The solid and dashed curves denote the results for $N = 50$ and 40, respectively. The thin dotted line denote $C_p/C_e = 0.647$ which is the value of C_p/C_e for $q = q_{\rm crit}$. For $q_i = 0.821$, we stopped the simulation at $t/\mu^{1/3} \approx 370$ because the BH reaches approximately stationary state. (b) The same as (a) but for the large initial spins $q_i = 0.878$, 0.933, 0.986, and 1.039 with $A = 0.005$. $C_p/C_e \approx 0.542$, 0.499, 0.460, and 0.422 at $t = 0$, respectively.

to a constant ≈ 0.700 for $q_i = 0.821$, ≈ 0.690 for $q_i = 0.801$, and ≈ 0.677 for $q_i = 0.781$, respectively, when $\eta \ll 1$ being achieved (we adopt the values of C_p/C_e when we stopped the simulations). We note that with a poor grid resolution, the value of C_p/C_e spuriously increases even for $\eta \ll 1$ because numerical dissipation tends to decrease the BH spin. This spurious variation is suppressed for the better grid resolutions (see also Fig. 7). The final values of C_p/C_e indicate the final spin $q_f \approx 0.675$, 0.688, and 0.705 for $q_i = 0.821$, 0.801, and 0.781, respectively, for which the BHs appear to be stable against any perturbation. It is worthy to note that the larger initial spin leads to the smaller final spin because a larger amount of gravitational-wave emission is enhanced during the evolution (see also Sec. V for the reason to this); the value of q_f is approximately written as $q_f = 2q_{\rm crit} - q_i$ for $q_i = 0.781$–0.821.

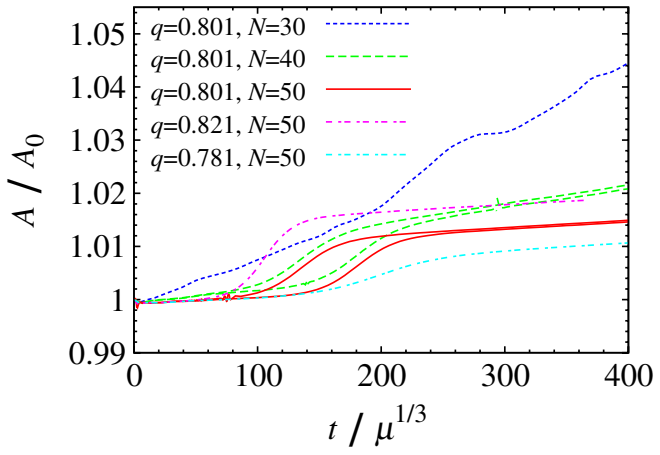

FIG. 7 (color online). The same as Fig. 6(a) but for the area of apparent horizon for $q_i = 0.801$ with $N = 30$ (dotted curve), 40 (dashed curves), and 50 (solid curves) and for $q_i = 0.781$ and 0.821 with $N = 50$ (lower and upper dot-dashed curves). A_0 is the initial value of the area, $\Omega_{d-2}\mu r_+$.

Figure 6(b) plots the evolution of C_p/C_e for $d = 6$ and for larger initial spins $q_i = 0.878$, 0.933, 0.986, and 1.039. As in the case of relatively small initial spins, the value of C_p/C_e increases with the evolution, and eventually settles to a constant after the BH is stabilized by gravitational radiation reaction. However, the final value of C_p/C_e depends only weakly on the initial spin, and hence, the final spin estimated from C_p/C_e is much larger than the value of $q_f = 2q_{\rm crit} - q_i$. Figure 6(b) shows that the fractional change of C_p/C_e after the BH is stabilized is smaller than that before the stabilization. This indicates that the fraction of spin-down is suppressed after the evolution of the nonlinear bar-mode deformation is saturated; again, this seems to be due to the fact that the evolution of the BHs after the saturation is achieved is determined by the property of the BH of spin slightly smaller than $q_{\rm crit}$. For $q_i = 0.878$–1.039, the final spin is relatively in a narrow range as $q_f \approx 0.65 - 0.61$. The results we found suggest that even for $q_i \gg 1$, the final spin q_f will not be close to zero, but moderately large as $\sim$0.6.

Qualitatively the same results for the final spin are obtained for $d = 7$. In this case, C_p/C_e relaxes to 0.72 ± 0.01 for $0.85 \lesssim q_i \lesssim 1$, implying that the final spin is in a

narrow range $q_f = 0.66$–0.69; even for $q_i \gg 1$, the final spin q_f will not be close to zero, but moderately large as ~ 0.65. The results of q_f for $d = 6$ and 7 together with the weak dependence of $q_{\rm crit}$ on d suggest that also for $d \geq 8$, the final spin will be moderately large $\gtrsim 0.6$–0.7.

The area of the BH has to increase as a result of spin-down [19]. Figure 7 plots the evolution of the horizon area for $d = 6$ and $q_i = 0.781$, 0.801, and 0.821 with $N = 50$. For $q_i = 0.801$, we plot the results for different grid resolutions. Figure 7 shows that the area indeed increases. As noted above, the area gradually increases with time even in the state of $\eta \ll 1$. This is partly due to numerical dissipation. Indeed, the error decreases significantly with improving the grid resolution; for $N = 50$, the spurious increase of the area seems to be negligible, and hence, we can determine the magnitude of the physical increase due to gravitational-wave emission. The area increases by $\approx$ 1.0%, 1.4%, and 1.8% for $q_i = 0.781$, 0.801, and 0.821, respectively. For the larger initial spins, the area increases more due to gravitational radiation reaction. A noteworthy fact is that the fractional increase of the area is much small than those for spin and mass energy of the BH (cf. Fig. 9).

V. PROPERTIES OF UNSTABLE BLACK HOLES

A. Conditions for spontaneous gravitational wave emission

The first law of BH thermodynamics allows us to determine the variation in the BH area δA as [32]

$$\frac{\kappa}{8\pi G_d}\delta A = -\Omega_{\rm H}\delta J + \delta E, \tag{49}$$

where κ is the surface gravity of the BH horizon, $\kappa = [2r_+^{d-3} + (d-5)\mu]/(2\mu r_+)$, which is positive for the BHs considered in this paper. δE and δJ are the variations of energy and angular momentum of the BH, and if the energy and angular momentum are carried away by gravitational waves, they should be negative. If we assume that gravitational waves of monochromatic wavelength are emitted, the following relation holds;

$$\delta E = \frac{\omega}{m}\delta J < 0. \tag{50}$$

Here, ω is the (real) angular frequency of the unstable mode [we regard it as $\omega = {\rm Re}(\omega_{\rm QN})$ in the following], and m is the azimuthal quantum number for which we set $m = 2$ because we focus on the bar-mode instability. The assumption of monochromatic wave emission is approximately correct because gravitational waves associated with the fundamental quasinormal mode are likely to be most strongly emitted. Indeed, Fig. 4 indicates that this is the case.

Substituting the relation (50) into Eq. (49), we obtain

$$\frac{\kappa}{8\pi G_d}\delta A = \left(\Omega_{\rm H} - \frac{\omega}{m}\right)|\delta J|. \tag{51}$$

This shows that only for $\Omega_{\rm H} > \omega/m$, δA becomes positive and the evolution by emission of gravitational waves is allowed without violating the area theorem [19]. This is the so-called superradiance condition [49]: If this condition holds, the energy flux of ingoing waves of an angular frequency $k = \omega - m\Omega_{\rm H}$ at the BH horizon becomes negative because $k < 0$.

This is a necessary condition that the unstable quasinormal mode should satisfy for the spontaneous emission of gravitational waves. However, this is not the sufficient condition. The superradiance is similar to secular instability in the terminology of an instability for rotating stars [47,50], because for the superradiance emission of gravitational waves from a stable BH with $\omega_I > 0$, one needs an artificial wave injection which satisfies the condition $k < 0$. We note that for the spontaneous emission of gravitational waves, one further needs to require the presence of a quasinormal mode with negative imaginary part for its angular frequency, $\omega_I < 0$.

To confirm that the superradiance condition is satisfied for the oscillation mode of unstable BHs, we first determine the real value of ω by performing the Fourier transformation of h_+ for the BHs. We identify the angular frequency at the spectrum peak as ω. Figure 8 plots the resulting values for $\omega/2$ (points) as well as $\Omega_{\rm H}$ (curves) as functions of q. We also plot the results for 5D BHs obtained in the previous paper [38]. This figure shows that the unstable modes with $\omega_I < 0$ always satisfy the superradiance condition $\Omega_{\rm H} > \omega/2$ and gravitational waves can

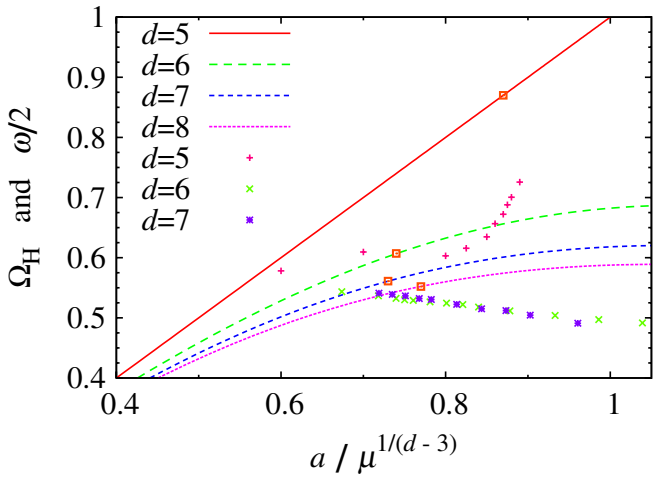

FIG. 8 (color online). $\Omega_{\rm H}$ as a function of $q = a/\mu^{1/(d-3)}$ for $d = 5$–8 (curves), and $\omega/m = \omega/2$ for selected values of the spin parameter for $d = 5$–7 (points). The units of the vertical axis are $\mu^{-1/(d-3)}$. We omit the points for $d = 8$ because they are located in the vicinity of the points for $d = 6$ and 7: The values of $\omega\mu^{1/(d-3)}/2$ are in a narrow range 0.49–0.55 for the chosen values of q and for $d = 6$–8. The squares on the curve of $\Omega_{\rm H}$ approximately denote the critical points for the onset of bar-mode instability (i.e., for spontaneous gravitational-wave emission).

be spontaneously emitted from the unstable BHs. A noteworthy point is that $\omega\mu^{1/(d-3)}(\approx 1.0$–$1.1)$ depends weakly on the spin q; for $d=6$, ω decreases slowly with q for $0.7 \le q \lesssim 1.1$ and for $d=7$ and 8, ω behaves in a manner similar to that of $d=6$ for $0.7 \le q \lesssim 1$.

In the following, we refer to the value of q, at which the real part of the quasinormal frequency becomes equal to the threshold frequency for the superradiance, as $q_{\rm SR}$. The superradiance condition is satisfied for the quasinormal modes when $q \gtrsim q_{\rm SR}$, where $q_{\rm SR} \approx 0.6$ for $d=5$, $q_{\rm SR} \approx 0.65$ for $d=6$, $q_{\rm SR} \approx 0.7$ for $d=7$, and $q_{\rm SR} \approx 0.75$ for $d=8$. Because the maximum value of $\Omega_{\rm H}\mu^{1/(d-3)}$ decreases as the number of d is increased and $\omega\mu^{1/(d-3)}$ for a given value of q depends weakly on d, the value of $q_{\rm SR}$ will increase as d is increased. This indicates that the critical value of spin, $q_{\rm crit}$, for the onset of the bar-mode instability (i.e., for the spontaneous gravitational-wave emission) will also increase with d for $d \ge 8$.

We note that Fig. 8 shows $\Omega_{\rm H} - \omega/m \ll \Omega_{\rm H}$ for $6 \le d \le 8$, and thus, the area increases only slightly even if a large amount of angular momentum is dissipated by gravitational-wave emission [see Eq. (51)]. This explains why the area increases only slightly (see Fig. 7) even when q changes by a large factor $\sim$0.1–0.2.

B. Mechanism of spin-down

Next, we consider the evolution of nondimensional spin parameter, q, as a result of gravitational-wave emission. The variation for this quantity, in the assumption of monochromatic gravitational-wave emission, is written as

$$\delta q = 8\pi G_d \mu^{-(d-2)/(d-3)} \Omega_{d-2}^{-1} \left(\delta J - \frac{2a}{d-3} \delta E \right) = -8\pi G_d \mu^{-(d-2)/(d-3)} \Omega_{d-2}^{-1} |\delta J| \left(1 - \frac{2}{d-3} \frac{a\omega}{m} \right), \tag{52}$$

or

$$\delta q = -\frac{|\delta J|}{J} q \left(1 - \frac{2}{d-3} \frac{a\omega}{m} \right). \tag{53}$$

As found from Eq. (51), the gravitational-wave emission is possible only for $\Omega_{\rm H} > \omega/m$. Thus,

$$1 - \frac{2}{d-3} \frac{a\omega}{m} > 1 - \frac{2}{d-3} a\Omega_{\rm H} = 1 - \frac{2}{d-3} \frac{a^2}{r_+^2 + a^2}. \tag{54}$$

Because $2/(d-3) \le 1$ and $a^2/(r_+^2 + a^2) < 1$ for any BH with $d \ge 5$, we find that δq is always negative for the superradiance mode. Thus, the unstable BHs have to spin down by gravitational radiation reaction and evolve toward a stable state, as we found in numerical simulation (cf. Fig. 6).

We quantitatively confirm from Eq. (53) that the spin-down of the unstable BHs is indeed due to gravitational-wave emission as shown in the following. Using a formula of gravitational-wave luminosity [51] (the Landau-Lifshitz pseudo tensor [40] also gives the same formula after partial integration), the luminosity of quadrupole gravitational waves ($l = |m| = 2$ mode) is written as

$$\frac{dE}{dt} = \frac{(\dot{h}_+^2 + \dot{h}_\times^2)\Omega_{d-2}}{16\pi G_d} \frac{(d-3)d}{(d-2)(d+1)} \mu^{(d-2)/(d-3)}. \tag{55}$$

For monochromatic gravitational waves with angular frequency ω, the luminosity may be rewritten as

$$\frac{dE}{dt} = \frac{\omega^2(h_+^2 + h_\times^2)\Omega_{d-2}}{16\pi G_d} \frac{(d-3)d}{(d-2)(d+1)} \mu^{(d-2)/(d-3)}. \tag{56}$$

In the following, we assume $h_+[\omega(t-r)] = h_\times[\omega(t-r) + \pi/2]$ (and set $h = \sqrt{h_+^2 + h_\times^2}$), and $\omega =$ const for simplicity, which approximately hold as mentioned before.

Rewriting Eq. (52) in the form of spin evolution as

$$\frac{dq}{dt} = -\frac{8\pi m G_d \mu^{-(d-2)/(d-3)}}{\omega\Omega_{d-2}} \left| \frac{dE}{dt} \right| \left(1 - \frac{2}{d-3} \frac{a\omega}{m} \right), \tag{57}$$

and integrating this equation, we may infer the spin-down history of a BH for the whole evolution process by

$$|\delta q(t)| = \int_0^t dt' \frac{m\omega h^2 d(d-3)}{2(d-2)(d+1)} \left(1 - \frac{2}{d-3} \frac{a\omega}{m} \right). \tag{58}$$

We also calculate dissipation history of the mass energy by

$$\delta E(t) = \int_0^t dt' \frac{dE}{dt}, \tag{59}$$

where we use Eq. (56) for dE/dt. We note that Eq. (52) is valid only for the case that deformation from a stationary BH solution is small. Thus, we here apply Eq. (58) only for the small values of $q_i - q_{\rm crit} < 0.1$ for which the maximum value of η is $\lesssim 0.15$ and the deformation remains in a weakly nonlinear level.

Figure 9 plots $|\delta q|$ and $\delta E/M$ as functions of t for $d=6$ and for $q_i = 0.821$, 0.801, and 0.781. Here, we assume that $a\omega = 1.05 q_i$ ($\omega\mu^{1/3} = 1.05$) taking into account the results shown in Fig. 8, and also neglect the dissipation of mass and spin of the BHs in computing the integrals of Eqs. (58) and (59), because the variation of these quantities gives a minor effect on δq and δE for $q_i - q_{\rm crit} < 0.1$; the error is likely to be less than 10%. As shown in Fig. 9, we obtain $\delta q_{\rm tot} \approx 0.14$, 0.11, and 0.07 for $q_i \approx 0.821$, 0.801, and 0.780, respectively, which agree with the results determined from the final value of C_p/C_e within the error $\Delta(\delta q) \approx 0.006$. Based on this good agreement, we conclude that the gravitational radiation reaction determines the spin-down of the unstable BHs and that in our simulations, the spin-down process is computed accurately. We

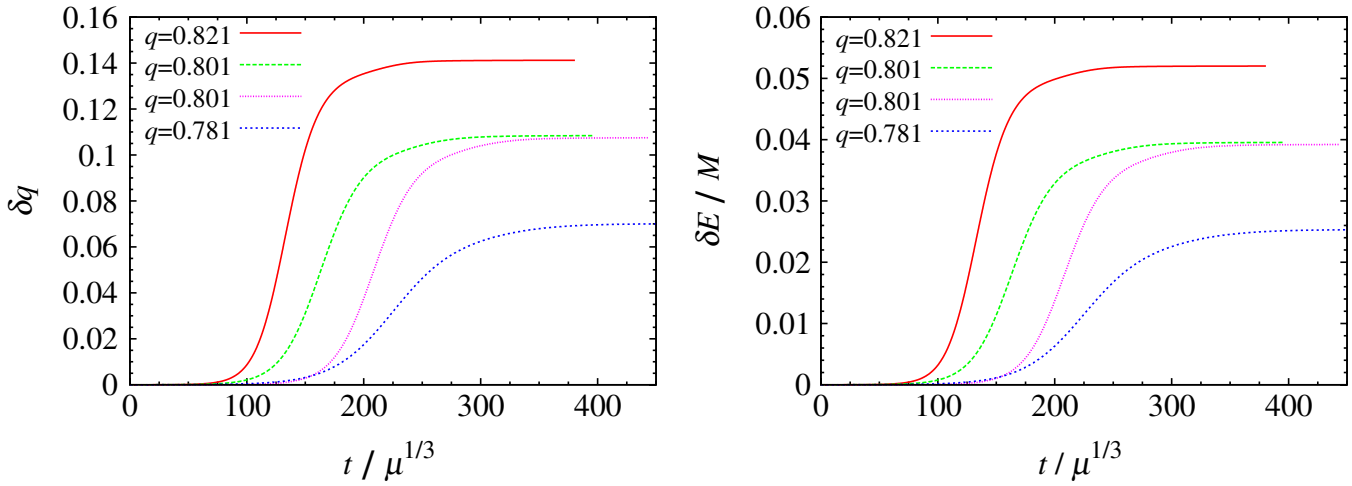

FIG. 9 (color online). $|\delta q|$ (left) and $\delta E/M$ (right) as functions of t for $d = 6$. The results for $q_i = 0.801$ with $A = 0.005$ and 0.02, and for $q_i = 0.781$ and 0.821 with $A = 0.02$ are displayed for $N = 50$. For $q_i = 0.821$, we stopped the simulation at $t/\mu^{1/3} \approx 370$ because the BH reaches approximately stationary state.

also note that the numerical results for the fractional increase of the area (cf. Fig. 7) agree well with that calculated from δq and δE obtained here.

As we have described above, the evolution process of an unstable BH with $q \lesssim 1$ is determined by gravitational radiation reaction. As far as the growth rate of the unstable mode is comparable with or smaller than the spin-down rate due to gravitational radiation reaction, the scenario presented here will be always correct. Figures 1(b) and 3(b) show that for the unstable BHs with $q_i \lesssim 1.1$, which have the growth time scale (τ) longer than $\pi/\Omega_{\rm H}$, this scenario holds. We, however, note that this scenario might not be valid for $q \gg 1$: If the growth time scale is too short (e.g., $\tau\omega \lesssim 1$), the BH could not emit a significant amount of gravitational waves in τ for spinning down, and as a result, it can achieve a state for which the deformation parameter is of order unity. Extrapolation of the results shown in Fig. 2(d) indeed suggests that for $q_i \gtrsim 1.6$, η may reach $\gtrsim 1$ for $d = 6$. For such case, gravitational radiation reaction may not prevent the growth of the bar-mode deformation, and then, highly nonlinear deformation may lead to fragmentation of the BH (in the classical argument, formation of a naked singularity may be the result), as discussed in [32]. In the present work, we have not pursued the possibility that η reaches ~ 1, because a long-term simulation for such an ultra spinning BH is not an easy task technically. We leave such a work for the future. In Sec. VI B, we speculate a condition for an ultra spinning BH to cause fragmentation.

Before closing this section, we note that the fraction of total radiated energy of gravitational waves is much smaller than that of angular momentum. The reason for this is that the following relation holds:

$$\frac{\delta J}{J_0} = \frac{d-2}{a\omega}\frac{\delta E}{M_0}. \tag{60}$$

Here, M_0 and J_0 are initial mass and angular momentum of a BH. For $d = 6$ and $q_i = 0.801$, for example, $\delta E/M_0$ is only $\approx 4\%$, whereas $\delta J/J_0$ is $\approx 20\%$. This significant angular-momentum dissipation is essential for the spin-down of the unstable BHs. It is worthy to note that the angular-momentum dissipation rate is even larger for the larger number of d for a given value of q because $\omega\mu^{1/(d-3)}$ depends weakly on d for the unstable BHs.

VI. SUMMARY AND DISCUSSIONS

A. Summary

We show by numerical-relativity simulation that BHs spinning sufficiently rapidly are unstable against nonaxisymmetric bar-mode deformation for $d = 6$, 7 and 8, as in the case $d = 5$ [38]. In this instability, gravitational waves are emitted spontaneously. The critical BH spin for the onset of the bar-mode instability is $q_{\rm crit} \approx 0.74$ for $d = 6$, ≈ 0.73 for $d = 7$, and ≈ 0.77 for $d = 8$, respectively. Thus, the critical value is smaller than unity, and depends only weakly on the dimensionality for $d \geq 6$. After the instability sets in, the degree of the bar-mode deformation increases exponentially with time, and eventually, it saturates. The saturation is caused by gravitational radiation reaction. For the larger initial spin, the growth time scale is shorter. The degree of the maximum deformation is larger for the larger initial value, approximately in proportional to $q_i - q_{\rm crit}$.

The unstable BHs emit gravitational waves significantly, and then, spin down, settling to a stable BH with $q < q_{\rm crit}$. The final value of the BH spin, $q_f (< q_{\rm crit})$, is smaller for the larger initial spin: For $d = 6$ with $q_i - q_{\rm crit} < 0.1$, the final spin is approximately written as $q_f = 2q_{\rm crit} - q_i$, and for $0.1 \lesssim q_i - q_{\rm crit} \lesssim 0.3$, the final spin is in a narrow range

$q_f \approx 0.6$–0.65. For $d = 7$, $q_f \approx 0.66$–0.69 for $0.85 \lesssim q_i \lesssim 1$. The smaller value of q_f for the larger initial spin q_i is due to a larger amount of gravitational-wave emission induced by the higher degree of the bar-mode deformation. The results for $q_i \sim 1$ indicate that for $q_i \gg 1$, the final spin is likely to be ~ 0.6 for $d = 6$ and ~ 0.65 for $d = 7$, if the BH settles to a stable state.

The dynamically unstable BHs satisfy two conditions. One is that a quasinormal mode satisfies a superradiance condition; the real part of the eigen angular frequency for the quasinormal mode, $\omega = \mathrm{Re}(\omega_{\mathrm{QN}})$, has to satisfy the condition $\omega < m\Omega_{\mathrm{H}}$. The other is that the imaginary part of the eigen angular frequency, $\omega_I = \mathrm{Im}(\omega_{\mathrm{QN}})$, is negative. The superradiance condition referred to here is satisfied not only for the dynamically unstable BHs but also for the stable BHs with the spin smaller than the critical value (q_{crit}). The minimum spin for which the real quasinormal frequency satisfies the superradiance condition, q_{SR}, is ~ 0.6 for $d = 5$, ~ 0.65 for $d = 6$, ~ 0.7 for $d = 7$, and ~ 0.75 for $d = 8$, respectively. Thus, q_{SR} increases with the number of d. This suggests that q_{crit} also increases with d for $d > 8$, because q_{crit} has to be larger than q_{SR} for the spontaneous gravitational-wave emission.

It is worthy to note that the dynamically unstable BHs we found always satisfy the above two conditions. If the superradiance condition were not satisfied, a BH could not emit gravitational waves spontaneously, even if it is dynamically unstable ($\omega_I < 0$). Probably, there would exist a mathematical proof for the relation $q_{\mathrm{crit}} \geq q_{\mathrm{SR}}$.

The value of q_{crit} depends weakly on the dimensionality for $d \geq 6$ as mentioned above. By contrast, this value is slightly larger for $d = 5$ ($q_{\mathrm{crit}} \approx 0.87$) [38] and absent for $d = 4$. This shows that properties of the spinning BHs are qualitatively similar for $d \geq 6$, whereas those for $d = 4$ and 5 have their intrinsic properties.

B. Axisymmetric vs nonaxisymmetric vs fragmentation instabilities

The critical spin for the onset of the bar-mode instability found in this paper is much smaller than that for the onset of axisymmetric instabilities [34,35], $q \geq 1.56$–1.80 for $d = 6$–9, respectively, (the minimum spins depend weakly on the dimensionality). Considering the analogy with the instabilities on rotating stars, we find that this is a quite reasonable consequence [47,52–54]: Rapidly and rigidly rotating stars can be unstable against axisymmetric instabilities (e.g., against toroid or ring formation) only for an extreme case in which the axial ratio of the polar axial length to the equatorial one is quite small (e.g., smaller than 0.171 for the incompressible fluid [52]). By contrast, a variety of nonaxisymmetric instabilities can set in even for the case that such ratio is not very small (for $\lesssim 0.58$, secular instabilities set in, and for $\lesssim 0.31$, dynamical instabilities set in for the incompressible fluid [47,53]). Also, the bar-mode instability occurs at the lowest critical spin among many other instabilities for most rotating stars; the bar-deformation is the most efficient way for decreasing total energy of the system. The bar-mode instability may be most relevant for any self-gravitating spheroidal objects spinning rapidly.

According to an estimate based on the BH thermodynamics by Emparan and Myers [32], the critical spin for the onset of a nonaxisymmetric instability is approximately unity, $q_{\mathrm{frag}} \approx 1$, irrespective of the number of d for $d \geq 6$. The assumption in their argument is that a rapidly spinning BH of area A_i will fragment into two nonspinning boosted BHs of the total area A_f which is larger than A_i. For the instability found in this paper for $q_i \lesssim 1$, the growth of the perturbation saturates at a weakly nonlinear level at $\eta \lesssim 0.5$, because gravitational-wave emission suppresses the further nonlinear growth. Thus, the fragmentation does not occur for $q_i \lesssim 1$. However, this does not imply that the fragmentation instability is not relevant for any spin. As we showed in Figs. 1 and 3, the growth time scale of the unstable mode depends strongly on the magnitude of the spin, and for $q \gtrsim 1$, it is shorter than a spin period of the BH, $\tau < 2\pi/\Omega_{\mathrm{H}}$. For $q \gg 1$, the growth time scale is likely to be even shorter. In such case, gravitational-wave emission will play a minor role and nonlinear growth will continue until a state of $\eta \sim 1$ is achieved, as discussed in Sec. V. Then, highly nonlinear bar-mode deformation may lead to a fragmentation of the BH due to the Gregory-Laflamme instability [33]. In the following, we infer how large initial spin is required for achieving the fragmentation focusing on the case $d = 6$.

As we showed in Figs. 1 and 3, the degree of bar-mode deformation for the unstable BHs increases exponentially with time as far as $\eta \lesssim 0.1$ as

$$\dot{\eta} = \frac{\eta}{\tau}, \tag{61}$$

where τ is a function of q, and for $d = 6$, $\tau^{-1} \approx C_\tau(q - q_{\mathrm{crit}})$ with $C_\tau \approx 0.51\mu^{-1/3}$. Gravitational radiation reaction plays a crucial role for suppressing the growth of the deformation. A nonlinearity associated with this effect plays an important role for larger values of η. We take into account this nonlinear effect by phenomenologically replacing τ to $\tau(1 + C_s\eta/2)$ where C_s is a constant of order unity. Because the amplitude of gravitational waves, h, is approximately written as $\eta/2$, we may assume the following approximate equation for the growth of gravitational-wave amplitude:

$$\dot{h} = \frac{h}{\tau(1 + C_s h)}. \tag{62}$$

Combining this relation with Eq. (57), we obtain

$$(1 + C_s h)\frac{dh^2}{dq} = -\frac{4}{\tau m\omega}\frac{(d-2)(d+1)}{(d-3)d}\left(1 - \frac{2}{d-3}\frac{a\omega}{m}\right)^{-1}. \tag{63}$$

This equation is valid only for $h \ll 1$, but in the following, we use it even for $h = O(1)$ to infer the maximum value of h as a function of q_i. For $d = 6$ with $m = 2$ and $q_{\rm crit} < q \lesssim 1.1$, this relation is approximately written as

$$(1 + C_s h)\frac{dh^2}{dq} \approx -C_\tau (q - q_{\rm crit})\frac{28}{9\omega}\left(1 - \frac{a\omega}{3}\right)^{-1}. \quad (64)$$

Because the factor, $1 - a\omega/3$, is a slowly varying function of q in the range 0.76–0.64 for $q = 0.7$–1.1, we assume that it is a constant and denote it by F^{-1}. In addition, we assume $\omega\mu^{1/3} \approx 1$ for simplicity. Using the approximate relation for C_τ, we finally obtain

$$(1 + C_s h)\frac{dh^2}{dq} \approx -1.6F(q - q_{\rm crit}). \quad (65)$$

Here, we assume that the maximum value of h ($h_{\rm peak}$) is achieved when the spin q reaches $q_{\rm crit}$ as a result of spin-down. Then, integrating Eq. (65) from $q = q_i$ to $q = q_{\rm crit}$ gives

$$h_{\rm peak}^2 + \frac{2C_s}{3}h_{\rm peak}^3 \approx 0.8F(q_i - q_{\rm crit})^2, \quad (66)$$

or, using $h_{\rm peak} \approx \eta_{\rm max}/2$,

$$\eta_{\rm max}^2 + \frac{C_s}{3}\eta_{\rm max}^3 \approx 3.2F(q_i - q_{\rm crit})^2. \quad (67)$$

Here, $3.2F$ is ≈ 4.2–5.0 for $q \approx 0.7$–1.1.

Equation (67) is indeed a good approximate relation for an appropriate choice of C_s. The solid curve of Fig. 2(d) is

$$\eta_{\rm max}^2 + 2\eta_{\rm max}^3 = 4(q_i - q_{\rm crit})^2, \quad (68)$$

and fits the numerical results well. It is found that for a high spin $q_i \gtrsim 0.9$, the nonlinearity associated with gravitational radiation reaction [the second term in the left-hand side of Eq. (68)] plays an important role in determining the value of $\eta_{\rm max}$.

Assuming that Eq. (68) is valid even for $q_i > 1.1$, we expect the maximum value of η and find that $\eta_{\rm max} \gtrsim 1$ for $q_i \gtrsim 1.6$ (note that the possible maximum value of η is 2). This suggests that the fragmentation may occur for an ultra spinning BH and the critical spin for the fragmentation, $q_{\rm frag}$, is $\gtrsim 1.6$; this predicted critical value is much larger than the value predicted in [32]. The critical spin for the onset of axisymmetric instabilities is fairly close to $q_{\rm frag}$ as $q_{\rm axis} \approx 1.56$ for $d = 6$ [35]. Therefore, for the ultra spinning case, the BH may fragment in a complicated manner. We note that for $\eta_{\rm max} \gtrsim 1$, several additional nonlinear effects will play an important role for the evolution of the deformed BH. For example, emission of gravitational waves with modes other than the lowest-order quadrupole mode could contribute to the spin-down and to suppressing the growth of the bar-mode instability. Thus, the critical spin for the fragmentation may be even larger than 1.6. Finally, we note that essentially the same argument holds also for $d \geq 7$.

C. Implications for mini black hole evolution

The bar-mode instability found in this paper changes the hypothetical picture for the evolution of a mini BH which may be formed in particle accelerators. It is natural to expect that most of the mini BH is formed for a large impact parameter, which is close to a critical value, $b_{\rm max}$, in two-particle collision, and that the BH should be rapidly spinning at its formation. In fact, analyses [55,56] for high-velocity two-particle collisions indicate that a BH can be formed for impact parameters such that the resulting BH is rapidly spinning with $q > 1$ for $d \geq 6$. To clarify this point, we first review the results of an analysis for high-velocity particle collision with the impact parameter b and with the energy of each incoming particle p [55,56]. For this phenomenon, the total mass energy and angular momentum of the system is $M = 2p$ and $J = bp$, respectively, assuming that the particles move with the speed of light. As in the case of the Myers-Perry BH of single spin, we define spin and mass parameters, a and μ, for this system using the same formulas as Eqs. (4) and (5), and then calculate nondimensional spin $q = a/\mu^{1/(d-3)}$. Table II shows the maximal impact parameters $b_{\rm max}/\mu^{1/(d-3)}$ for the apparent horizon formation obtained in [56] and the corresponding value of the spin $q = q_{\rm max}$ for $d = 5$–8. The value of $q_{\rm max}$ is larger than unity for $d = 6$–8, and thus, the resulting BH is likely to be rapidly spinning so that it can be subject to the dynamical bar-mode instability.[1]

The phenomenology of a mini BH formed in particle accelerators is determined by two time scales: One is the time scale of gravitational-wave emission $\tau_{\rm GW} \sim 1/|\omega_I|$. The other is the time scale of Hawking radiation $\tau_{\rm H}$. For convenience, we denote these time scales in terms of the Planck mass $m_{\rm P}$. Among several manners of defining the Planck mass (summarized in [4]), we adopt the definition as

$$m_{\rm P} = \left[\frac{(2\pi)^{d-4}}{4\pi G_d}\right]^{1/(d-2)}. \quad (69)$$

Then, the Planck time is defined by $\tau_{\rm P} := 1/m_{\rm P}$ in the natural units.

The time scale of gravitational-wave emission is written as

$$\tau_{\rm GW} = C_{\rm GW}\tau_{\rm P}\left(\frac{M_0}{m_{\rm P}}\right)^{1/(d-3)}, \quad (70)$$

where M_0 is the initial BH mass. If the formed BH is stable,

[1] In this analysis, we assume that the mass and angular momentum for the formed BH are equal to those of the system for simplicity. However, this is not likely to be the case because gravitational waves should be significantly emitted during the collision. The value of $q_{\rm max}$ is nothing but a roughly approximated value. As we showed in this paper, angular momentum will be more efficiently emitted by gravitational waves than energy. Thus, the resulting spin could be smaller than $q_{\rm max}$ in reality.

TABLE II. The values of maximal impact parameter $b_{\rm max}/\mu^{1/(d-3)}$ for the apparent horizon formation obtained in [56] and the corresponding nondimensional spin of the system, $q_{\rm max}$.

d	5	6	7	8
$b_{\rm max}/\mu^{1/(d-3)}$	1.24	1.47	1.59	1.66
$q_{\rm max}$	0.93	1.47	1.98	2.50

$\tau_{\rm GW}$ should be defined by $1/|\omega_I|$, and the coefficient is

$$C_{\rm GW} = \frac{2\pi}{\omega_I}\left[\frac{2}{\pi(d-2)\Omega_{d-2}\mu}\right]^{1/(d-3)}. \quad (71)$$

For the 6D head-on collision ($q = 0$), for example, $C_{\rm GW} \approx 3.8$ [57], and this factor depends weakly on the dimensionality as long as $q = 0$. For spinning BHs, it becomes larger, and $C_{\rm GW} \gg 1$ for $q \sim q_{\rm crit}$ as found in the present paper; practically $C_{\rm GW} = O(100)$, if gravitational radiation reaction is taken into account.

If the value of q is further increased to be $q > q_{\rm crit}$, the value of $C_{\rm GW}$ should be approximately written as

$$C_{\rm GW} = \frac{2\pi}{|\omega_I|}\left[\frac{2}{\pi(d-2)\Omega_{d-2}\mu}\right]^{1/(d-3)} + C_{\rm GW0}, \quad (72)$$

where the first term in the right-hand side is associated with the growth time scale for the bar-mode deformation and the second one is the time scale of damping after the saturation is achieved, which is approximately equal to $C_{\rm GW}$ in Eq. (71) for $q \lesssim q_{\rm crit}$ and thus of order 10–10^2 [cf. Fig. 2(b) and 2(c)]. The first term is comparable to the second term for $q_{\rm crit} < q \lesssim q_{\rm crit} + 0.1$ but the second term dominates for the larger value of q.

The time scale of Hawking radiation is

$$\tau_{\rm H} = C_{\rm H}\tau_{\rm P}\left(\frac{M_0}{m_{\rm P}}\right)^{(d-1)/(d-3)}, \quad (73)$$

where $C_{\rm H}$ is a q-dependent constant and determined taking into account all emission processes (i.e., emission of scalar, spinor, vector particles and gravitons). For the Schwarzschild case, $C_{\rm H}$ can be evaluated using numerical results of the greybody factor [7]; e.g., $C_{\rm H} \approx 1.7$ for $d = 6$. The greybody factors for spinning BHs are studied for brane spacetimes [8–11] whereas those for bulk gravitons have never been completely evaluated (but see [12]). The general tendency is that the emission rate is enhanced significantly as the value of q or d is increased: The luminosity for $q \sim 1$ is $\sim$100 times as large as that for $q = 0$ (e.g., [10]). The angular momentum emission rate is more significantly enhanced as the spin is increased, indicating that a rapidly spinning BH spins down in a short time scale. Thus, strictly speaking, we should take into account two time scales: One is the evaporation time scale $\tau_{\rm H}$ and the other is the spin-down time scale referred to as $\tau_{\rm Hs}$ (i.e., the time scale in which the BH spin is decreased to become $q = q_{\rm crit}$). Reference [10] shows that for $q \sim 1$, $\tau_{\rm Hs} \ll \tau_{\rm H}$: $\tau_{\rm Hs}$ is shorter than $\tau_{\rm H}$ typically by a factor of 10.

The ratio of $\tau_{\rm H}$ to $\tau_{\rm GW}$ is

$$\frac{\tau_{\rm H}}{\tau_{\rm GW}} = \frac{C_{\rm H}}{C_{\rm GW}}\left(\frac{M_0}{m_{\rm P}}\right)^{(d-2)/(d-3)}, \quad (74)$$

and proportional to $M_0^{(d-2)/(d-3)}$ where $1 < (d-2)/(d-3) \le 4/3$ for $d \ge 6$. Thus, the ratio depends moderately on M_0 for $m_{\rm P} < M_0 \lesssim 10 m_{\rm P}$. On the other hand, $C_{\rm H}/C_{\rm GW}$ are in the range $\sim 10^{-3}$–1, depending strongly on the spin. This implies that the evolution of a mini BH formed after a particle collision depends strongly on the spin q (or equivalently, the impact parameter b).

Now, we discuss the phenomenology of a mini BH assuming that $m_{\rm P} = 1$ TeV and $M_0 = 10$ TeV $= 10 m_{\rm P}$, which are plausible values in TeV-gravity scenarios and in LHC. Note that the scenario is qualitatively unchanged as far as $M_0 \lesssim 10^2 m_{\rm P}$. As a specific example, we further fix $d = 6$ in the following. For $M_0 = 10 m_{\rm P}$, $\tau_{\rm GW} \approx 8\tau_{\rm P}$ and $\tau_{\rm H} \approx 80\tau_{\rm P} \gg \tau_{\rm GW}$ for $q = 0$. As the value of q is increased from $q = 0$, $\tau_{\rm GW}$ becomes longer and $\tau_{\rm H}$ shorter. Thus, two time scales, $\tau_{\rm GW}$ and $\tau_{\rm H}$, become identical, $\tau_{\rm GW} = \tau_{\rm H}$, at a value of $q = q_{\rm eq}$. The result in this paper indicates $q_{\rm eq} < q_{\rm crit}$, because $\tau_{\rm GW}$ becomes very long ($C_{\rm GW}$ is of order 100) for $q \sim q_{\rm crit}$.

Then, the phenomenology is classified into three types depending on the spin q; (i) $0 \le q \lesssim q_{\rm eq}$, (ii) $q_{\rm eq} \lesssim q < q_{\rm frag}$, and (iii) $q \ge q_{\rm frag}$. Here, we assume a hypothetical critical value for the onset of fragmentation as $q_{\rm frag} \gtrsim 1.6$ following the estimate in Sec. VI B, although it is not clear whether the fragmentation really occurs. Because of the high value of q, the fragmentation will proceed in a time scale of order $M_0^{1/(d-3)} \sim \tau_{\rm H} \ll \tau_{\rm GW}$, if it occurs.

For the case (i), the standard hypothetical picture of BH evaporation holds; a formed BH emits gravitational waves and settles to a stationary state in a short time scale. Then, it will be evaporated by Hawking radiation. The formed BH is spinning, but not very rapidly, and the effect of the energy loss and spin-down by gravitational radiation reaction plays a minor role. The spin-down will proceed primarily by Hawking radiation, and finally, a nearly nonspinning BH will be evaporated. This type of BH formation and evaporation will not be a dominant process in particle accelerators, because a mini BH with such a small spin ($q < q_{\rm eq} < q_{\rm crit}$) or with a small impact parameter will not be formed frequently; the formation rate will be by a factor of $(q_{\rm eq}/q_{\rm max})^2$ smaller than the total.

For the case (ii), the BH will not be relaxed to a stable state by gravitational-wave emission, because of its long emission time scale. Such a nonstationary BH will start radiating quantum particles while emitting gravitational waves, and the signal of the quantum radiation in this phase is likely to be different from the idealized Hawking radiation (which is the result only from a stationary, axisymmetric BH). Because a BH with a large initial spin reaches a highly deformed state, non-

Hawking-type quantum radiation will be enhanced for the higher spin. Obviously, an improved analysis for predicting the spectrum of the quantum radiation is required. Assuming that the spin-down time scale by the quantum radiation is shorter than the evaporation time scale as in the Hawking radiation [10], the BH spin will subsequently become smaller than $q_{\rm crit}$ after the substantial quantum radiation, and thus, the BH relaxes eventually to a stable, quasistationary, axisymmetric state and will stop emitting gravitational waves. After the condition $q < q_{\rm crit}$ is achieved, the quantum radiation process will be identical to the ordinary Hawking radiation.

For the case (iii), the time scale for the growth of bar-mode deformation and subsequent fragmentation is likely to be of order $\sim M_0^{1/(d-3)}$. This may be as short as $\tau_{\rm Hs}$. If fragmentation occurs, a rapidly spinning BH is likely to change to two slowly spinning BHs before the quantum (Hawking) radiation becomes the dominant dissipation process. A supportive evidence for this possibility is that the apparent horizon formed in particle collisions takes a peanut shape for $b \approx b_{\rm max}$ as shown in Figs. 5 and 6 of [56], which indicates that gravity combining the two particles is weak. If the fragmentation occurs (the BH horizon pinches off) because of quantum-gravity effect, two boosted BHs will be the outcome (binary will not be the result for $d \geq 5$). Thus, the Hawking radiation from the two boosted BHs may be observed subsequently, as two jets in particle accelerators. Here, we note that the two time scales, $M_0^{1/(d-3)}$ and $\tau_{\rm Hs}$, may be as short as the Planck time $\tau_{\rm P}$ for $M_0 \approx 10 m_{\rm P}$, and thus, such a (semi) classical phenomena may be veiled by quantum-gravity effects in LHC.

D. Issues for the future

The present paper reports the results for the stability of rapidly spinning BHs against bar-mode deformation. We analyzed the BHs only with the spin $q \lesssim 1.15$ and did not study for the ultra spinning case with $q \gtrsim 1.5$ because it is not technically easy to perform a long-term simulation for such BHs. As discussed above, the evolution of the ultra spinning BHs may be qualitatively different from that for $q \lesssim 1$. Furthermore, such ultra spinning BHs may be the frequent outcomes, if the TeV-gravity hypothesis is correct. Clarifying the evolution of the ultra spinning BHs is obviously an important issue left for the future.

The stability of black rings against bar-mode deformation is one of the interesting issues. The analytic solutions for the black rings are found in five dimensions [26], and numerical-relativity simulation in a similar manner to that in this paper may be possible. The black rings always have a high spin with $q > q_{\rm crit}$ for $d = 5$. Perhaps, they are also unstable against bar-mode deformation and evolve as a result of gravitational radiation reaction as far as q is not extremely large; if the spin is very large, fragmentation may occur.

In the present paper, we start simulations in a highly idealized situation; we prepare nearly stationary, axisymmetric BHs and evolve them approximately in a quasistationary manner. In particle accelerators, however, the situation will be highly different. The rapidly spinning BHs after the particle collision will be highly nonstationary and nonaxisymmetric. Such BHs may evolve qualitatively in a similar manner to that in the present analysis, but quantitative properties on the evolution process will be significantly different. To clarify the formation and evolution of such BHs, it is necessary to perform a simulation started from high-velocity two-BH collision. Our goal is to successfully perform this simulation and to clarify the possible outcome in this setting.

ACKNOWLEDGMENTS

We thank T. Tanaka, T. Shiromizu, M. Sasaki, and H. Kodama for discussions. H. Y. thanks also V. P. Frolov and A. Zelnikov for comments. Numerical computations were in part performed on the NEC-SX9 at CfCA in National Astronomical Observatory of Japan and on the NEC-SX8 at Yukawa Institute for Theoretical Physics in Kyoto University. This work was in part supported by Grant-in-Aid for Scientific Research (21340051) and by Grant-in-Aid for Scientific Research on Innovative Area (20105004) of the Japanese MEXT. H. Y. is supported by JSPS.

[1] N. Arkani-Hamed, S. Dimopoulos, and G. R. Dvali, Phys. Lett. B **429**, 263 (1998); I. Antoniadis, N. Arkani-Hamed, S. Dimopoulos, and G. R. Dvali, *ibid.* **436**, 257 (1998).
[2] L. Randall and R. Sundrum, Phys. Rev. Lett. **83**, 3370 (1999).
[3] T. Banks and W. Fischler, arXiv:hep-th/9906038; S. Dimopoulos and G. Landsberg, Phys. Rev. Lett. **87**, 161602 (2001).
[4] S. B. Giddings and S. Thomas, Phys. Rev. D **65**, 056010 (2002).
[5] M. Cavaglia, Int. J. Mod. Phys. A **18**, 1843 (2003); P. Kanti, Int. J. Mod. Phys. A **19**, 4899 (2004); S. Hossenfelder, arXiv:hep-ph/0412265; P. Kanti, Lect. Notes Phys. **769**, 387 (2009).
[6] S. W. Hawking, Commun. Math. Phys. **43**, 199 (1975).
[7] P. Kanti and J. March-Russell, Phys. Rev. D **66**, 024023 (2002); **67**, 104019 (2003); C. M. Harris and P. Kanti, J. High Energy Phys. 10 (2003) 014; A. S. Cornell, W. Naylor, and M. Sasaki, J. High Energy Phys. 02 (2006) 012; V. Cardoso, M. Cavaglia, and L. Gualtieri, Phys. Rev.

Lett. **96**, 071301 (2006); **96**, 219902(E) (2006).
[8] D. Ida, K. Y. Oda, and S. C. Park, Phys. Rev. D **67**, 064025 (2003); **69**, 049901(E) (2004).
[9] D. Ida, K. Y. Oda, and S. C. Park, Phys. Rev. D **71**, 124039 (2005).
[10] D. Ida, K. Y. Oda, and S. C. Park, Phys. Rev. D **73**, 124022 (2006).
[11] C. M. Harris and P. Kanti, Phys. Lett. B **633**, 106 (2006); G. Duffy, C. Harris, P. Kanti, and E. Winstanley, J. High Energy Phys. 09 (2005) 049.
[12] P. Kanti, H. Kodama, R. A. Konoplya, N. Pappas, and A. Zhdenko, Phys. Rev. D **80**, 084016 (2009).
[13] R. Emparan, G. T. Horowitz, and R. C. Myers, Phys. Rev. Lett. **85**, 499 (2000); V. P. Frolov and D. Stojkovic, Phys. Rev. D **67**, 084004 (2003); **68**, 064011 (2003); M. Cavaglia, Phys. Lett. B **569**, 7 (2003); D. Stojkovic, Phys. Rev. Lett. **94**, 011603 (2005).
[14] U. Sperhake, V. Cardoso, F. Pretorius, E. Berti, and J. A. González, Phys. Rev. Lett. **101**, 161101 (2008).
[15] M. Shibata, H. Okawa, and T. Yamamoto, Phys. Rev. D **78**, 101501(R) (2008).
[16] U. Sperhake, V. Cardoso, F. Pretorius, E. Berti, T. Hinderer, and N. Yunes, Phys. Rev. Lett. **103**, 131102 (2009).
[17] M. W. Choptuik and F. Pretorius, Phys. Rev. Lett. **104**, 111101 (2010).
[18] S. B. Giddings and V. S. Rychkov, Phys. Rev. D **70**, 104026 (2004).
[19] S. W. Hawking and G. F. R. Ellis, *The Large Scale Structure of Space-Time* (Cambridge University Press, Cambridge, England, 1973); R. M. Wald, *General Relativity* (The University of Chicago Press, Chicago and London, 1984).
[20] W. H. Press and S. A. Teukolsky, Astrophys. J. **185**, 649 (1973).
[21] E. W. Leaver, Proc. R. Soc. A **402**, 285 (1985).
[22] B. F. Whiting, J. Math. Phys. (N.Y.) **30**, 1301 (1989).
[23] V. P. Frolov and I. D. Novikov, *Black Hole Physics* (Kluwer Academic Publishers, Norwell, MA, 1998), Chap. 4.
[24] Y. Morisawa and D. Ida, Phys. Rev. D **69**, 124005 (2004).
[25] R. C. Myers and M. J. Perry, Ann. Phys. (N.Y.) **172**, 304 (1986).
[26] R. Emparan and H. S. Reall, Living Rev. Relativity **11**, 6 (2008).
[27] H. Iguchi and T. Mishima, Phys. Rev. D **75**, 064018 (2007); **78**, 069903(E) (2008); J. Evslin and C. Krishnan, Classical Quantum Gravity **26**, 125018 (2009).
[28] H. Elvang and P. Figueras, J. High Energy Phys. 05 (2007) 050.
[29] A. A. Pomeransky and R. A. Sen'kov, arXiv:hep-th/0612005; K. Izumi, Prog. Theor. Phys. **119**, 757 (2008); H. Elvang and M. J. Rodriguez, J. High Energy Phys. 04 (2008) 045.
[30] H. Yoshino and Y. Nambu, Phys. Rev. D **70**, 084036 (2004).
[31] H. Yoshino and T. Shiromizu, Phys. Rev. D **76**, 084021 (2007).
[32] R. Emparan and R. C. Myers, J. High Energy Phys. 09 (2003) 025.
[33] R. Gregory and R. Laflamme, Phys. Rev. Lett. **70**, 2837 (1993).
[34] O. J. C. Dias, P. Figueras, R. Monteiro, J. E. Santos, and R. Emparan, Phys. Rev. D **80**, 111701(R) (2009).
[35] K. Murata, T. Tanahashi, and T. Tanaka (unpublished).
[36] K. Murata and J. Soda, Prog. Theor. Phys. **120**, 561 (2008); H. Kodama, R. A. Konoplya, and A. Zhidenko, Phys. Rev. D **81**, 044007 (2010); O. J. C. Dias, P. Figueras, R. Monteiro, H. S. Reall, and J. E. Santos, arXiv:1001.4527.
[37] V. Cardoso and O. J. C. Dias, J. High Energy Phys. 04 (2009) 125; V. Cardoso, O. J. C. Dias and J. V. Rocha, J. High Energy Phys. 01 (2010) 021.
[38] M. Shibata and H. Yoshino, Phys. Rev. D **81**, 021501(R) (2010).
[39] T. Yamamoto, M. Shibata, and K. Taniguchi, Phys. Rev. D **78**, 064054 (2008).
[40] H. Yoshino and M. Shibata, Phys. Rev. D **80**, 084025 (2009).
[41] M. Alcubierre, S. Brandt, B. Bruegmann, D. Holz, E. Seidel, R. Takahashi, and J. Thornburg, Int. J. Mod. Phys. D **10**, 273 (2001); M. Shibata, Prog. Theor. Phys. **104**, 325 (2000).
[42] M. Shibata and T. Nakamura, Phys. Rev. D **52**, 5428 (1995); T. W. Baumgarte and S. L. Shapiro, Phys. Rev. D **59**, 024007 (1998).
[43] M. Zilhao, H. Witek, U. Sperhake, V. Cardoso, L. Gualtieri, C. Herdeiro, and A. Nerozzi, Phys. Rev. D **81**, 084052 (2010).
[44] M. Campanelli, C. O. Lousto, P. Marronetti, and Y. Zlochower, Phys. Rev. Lett. **96**, 111101 (2006); J. G. Baker, J. Centrella, D.-I. Choi, M. Koppitz, and J. van Meter, Phys. Rev. Lett. **96**, 111102 (2006).
[45] W. Krivan and R. H. Price, Phys. Rev. D **58**, 104003 (1998).
[46] W. Press, B. P. Flannery, S. Teukolosky, and W. T. Vetterling, *Numerical Recipies* (Cambridge University Press, Cambridge, England, 1986).
[47] S. Chandrasekhar, *Ellipsoidal Figures of Equilibrium* (Dover, New York, 1969).
[48] B. Brügmann, J. A. Gonzalez, M. Hannam, S. Husa, U. Sperhake, and W. Tichy, Phys. Rev. D **77**, 024027 (2008).
[49] S. A. Teukolsky and W. H. Press, Astrophys. J. **193**, 443 (1974).
[50] J. L. Friedman and B. F. Schutz, Astrophys. J. **222**, 281 (1978).
[51] V. Cardoso, O. J. C. Dias, and J. P. S. Lemos, Phys. Rev. D **67**, 064026 (2003).
[52] S. Chandrasekhar, Astrophys. J. **147**, 334 (1967); J. M. Bardeen, Astrophys. J. **167**, 425 (1971); Y. Eriguchi and D. Sugimoto, Prog. Theor. Phys. **65**, 1870 (1981).
[53] Y. Eriguchi and I. Hachisu, Prog. Theor. Phys. **67**, 844 (1982).
[54] V. Cardoso and L. Gualtieri, Classical Quantum Gravity **23**, 7151 (2006).
[55] H. Yoshino and Y. Nambu, Phys. Rev. D **67**, 024009 (2003).
[56] H. Yoshino and V. S. Rychkov, Phys. Rev. D **71**, 104028 (2005); **77**, 089905(E) (2008).
[57] H. Yoshino, T. Shiromizu, and M. Shibata, Phys. Rev. D **72**, 084020 (2005).